Inflammation switches the differentiation program of Ly6C^{hi} monocytes from antiinflammatory macrophages to inflammatory dendritic cells in the colon

Aymeric Rivollier, Jianping He, Abhisake Kole, Vassilis Valatas, and Brian L. Kelsall

Mucosal Immunobiology Section, Laboratory of Molecular Immunology, National Institute of Allergy and Infectious Diseases, National Institutes of Health, Bethesda, MD 20892

Dendritic cells (DCs) and macrophages (MPs) are important for immunological homeostasis in the colon. We found that F4/80^{hi}CX3CR1^{hi} (CD11b^{+}CD103^{-}) cells account for 80% of mouse colonic lamina propria MHC-II^{hi} cells. Both CD11c^{+} and CD11c^{-} cells within this population were identified as MPs based on multiple criteria, including an MP transcriptome revealed by microarray analysis. These MPs constitutively released high levels of IL-10 at least partially in response to the microbiota via an MyD88-independent mechanism. In contrast, cells expressing low to intermediate levels of F4/80 and CX3CR1 were identified as DCs based on phenotypic and functional analysis and comprise three separate CD11c^{hi} cell populations: CD103^{+}CX3CR1^{-}CD11b^{-} DCs, CD103^{+}CX3CR1^{-}CD11b^{+} DCs, and CD103^{-}CX3CR1^{int}CD11b^{+} DCs. In noninflammatory conditions, Ly6C^{hi} monocytes (MOs) differentiated primarily into CD11c^{+} but not CD11c^{-} MPs. In contrast, during colitis, Ly6C^{hi} MOs massively invaded the colon and differentiated into proinflammatory CD103^{-}CX3CR1^{int}CD11b^{+} DCs, which produced high levels of IL-12, IL-23, iNOS, and TNF. These findings demonstrate the dual capacity of Ly6C^{hi} blood MOs to differentiate into either regulatory MPs or inflammatory DCs in the colon and that the balance of these immunologically antagonistic cell types is dictated by microenvironmental conditions.

CORRESPONDENCE
Brian L. Kelsall:
bkelsall@niaid.nih.gov

Abbreviations used: cLP, colonic LP; DTR, DTx receptor; DTx, diphtheria toxin; GF, germ free; IEC, intestinal epithelial cell; LP, lamina propria; MLN, mesenteric LN; MNP, mononuclear phagocyte; MO, monocyte; MP, macrophage; mRNA, messenger RNA; SI, small intestine; SPF, specific pathogen free.

Immune responses in the intestine need to be tightly regulated, particularly in the colon where the ability to combat pathogenic microbes must be balanced with the need to prevent exuberant inflammatory responses to the large pool of diverse commensal microorganisms. How this occurs is not yet clear; however, there is increasing evidence that specialized gut-resident DCs and macrophages (MPs), in addition to providing innate defense against both pathogenic and commensal microorganisms, are directly involved in driving regulatory responses. These include the differentiation, expansion, and maintenance of regulatory T cell (T reg cell) populations and the induction of IgA against commensal bacteria (Manicassamy and Pulendran, 2009). However, there is less consensus regarding the definition and functions of any one of several specialized MP and DC populations, particularly because the inconsistent use of an ever increasing number of surface markers has resulted in new levels of complexity.

We and others originally defined DCs in the intestine based on the traditional lymphoid organ DC markers CD11c, CD8α, and CD11b (Iwasaki and Kelsall, 1999, 2001; Chirdo et al., 2005). More recently, a new organizational scheme of intestinal DC and MP populations has been proposed based on their expression of the nonoverlapping markers CD103 (αE integrin) and CX3CR1 (fractalkine receptor; Schulz et al., 2009). CD103^{+} DCs were identified in the small intestine (SI) lamina propria (LP),

A. Rivollier's present address is Immunology Section, Dept. of Experimental Medical Science, Lund University, 22184 Lund, Sweden.
V. Valatas' present address is Dept. of Gastroenterology, University Hospital of Heraklion, Heraklion GR-71100, Crete, Greece.

The Rockefeller University Press $30.00
J. Exp. Med. Vol. 209 No. 1 139-155
www.jem.org/cgi/doi/10.1084/jem.20101387

mesenteric LNs (MLNs), and Peyer's patches of mice (Johansson-Lindbom et al., 2005) and recently in human colonic tissues (Jaensson et al., 2008). $CD103^+$ DCs have a high capacity to produce the vitamin A metabolite retinoic acid and TGF-β (Coombes et al., 2007), which gives them enhanced ability to drive the expression of the gut-homing molecules α4β7 and CCR9 on naive T cells during priming (Iwata et al., 2004; Jaensson et al., 2008). They also have been shown to induce the de novo differentiation of $foxp3^+$ T reg cells (Coombes et al., 2007; Sun et al., 2007) and contribute to IgA^+ B cell differentiation from naive precursors in vitro (Mora et al., 2006). In the SI LP, $CD103^+$ DCs are predominantly $CD11b^+CD8\alpha^-$ (Coombes et al., 2007; Denning et al., 2007b; Sun et al., 2007), appear to be the main, if not the only, DC population that constitutively migrates to the MLNs via a CCR7-dependent mechanism, and are critical for the induction of oral tolerance, as well as for the suppression of colitis development by T reg cells (Annacker et al., 2005; Worbs et al., 2006; Bogunovic et al., 2009; Schulz et al., 2009). $CD103^+$ DCs do not express CX3CR1 and, whether they are $CD11b^+$ or $CD11b^-$, expand in response to Flt3-L and GM-CSF and are generated by adoptively transferred pre-DCs (Bogunovic et al., 2009; Varol et al., 2009).

In contrast, $CX3CR1^+$ cells do not express CD103 and were initially described as DCs in the terminal ileum, extending dendrites between epithelial cells (intestinal epithelial cells [IECs]) to actively take up bacteria and soluble antigens from the intestinal lumen. These cells were thus proposed to play a key role in the capture and transport of intestinal antigens to the MLNs (Rescigno et al., 2001; Niess et al., 2005; Vallon-Eberhard et al., 2006; Hapfelmeier et al., 2008; Bogunovic et al., 2009; Schulz et al., 2009). However, the identity of the $CD11c^+CX3CR1^+$ cells as bona fide DCs has been challenged by studies in the SI LP that illustrated their MP-like vacuolar system (Bogunovic et al., 2009) and their poor ability to drive naive T cell stimulation and differentiation (Bogunovic et al., 2009; Schulz et al., 2009), as well as their inability to migrate to draining MLNs (Schulz et al., 2009). In addition, $CX3CR1^+$ cells have a different ontogeny in the intestine, relative to $CD103^+$ DCs, and appear to be derived from $Gr\text{-}1^{hi}$ monocytes (MOs) in an M-CSF–dependent manner (Bogunovic et al., 2009; Varol et al., 2009). Both pro- and antiinflammatory properties have been documented for $CX3CR1^+$ cells in the LP. $CX3CR1^+$ cells seem to play a critical role in the oral tolerance induction process, by expanding $foxp3^+$ T reg cells in the SI LP, subsequent to their priming in the MLNs (Hadis et al., 2011) but also support inflammatory immune responses under normal conditions and in both innate and $CD45RB^{hi}$ $CD4^+$ T cell transfer colitis models (Varol et al., 2009; Niess and Adler, 2010). Therefore, whether LP $CX3CR1^+$ cells are MPs or DCs and whether these cells play pro- or antiinflammatory functions require further clarification. One key point to consider when addressing this question is the fact that LP $CX3CR1^+$ cells represent a heterogeneous group of cells expressing low to high levels of CX3CR1 (Schulz et al., 2009; Varol et al., 2009).

Independently of CX3CR1 expression, several intestinal MP populations have also been characterized. In the human, two $CD68^+$ MP populations coexist in the intestine of patients with inflammatory bowel disease: a steady-state $CD14^-$ inflammatory anergic population that neither expresses innate response receptors (Rogler et al., 1998; Smith et al., 2001; Smythies et al., 2005) nor produces proinflammatory cytokines in response to an array of inflammatory stimuli but retains avid phagocytic and bactericidal activity (Smythies et al., 2005) and an additional $CD14^+$ proinflammatory population that accumulates in patients with Crohn's disease and contributes to the pathogenesis of this disease (Rugtveit et al., 1997; Kamada et al., 2008). In the mouse SI, $CD11c^-F4/80^+CD11b^+$ MPs express IL-10, induce the differentiation of foxp3+ T reg cells in the presence of exogenous TGF-β, and suppress the differentiation of Th17 by $CD11c^+CD11b^+$ DCs in vitro (Denning et al., 2007b). In the mouse colon, MPs, defined as $CD11c^{-/lo}F4/80^+CD11b^+$ cells, seem to represent a heterogeneous pool of cells, and discrepancies in the literature regarding their pro- or antiinflammatory properties in the steady-state and during colitis remain to be resolved (Platt et al., 2010; Takada et al., 2010). Therefore, the identification and characterization of the colonic LP (cLP) MP pool is only beginning to be unveiled in the mouse, and the pro- or antiinflammatory nature of these cells is still unclear.

To clarify the discrepancies in the definition, function, and origin of mucosal DCs and MPs, we undertook experiments in mice to extensively phenotypically and functionally characterize DC and MP populations in the colon during steady-state conditions and during inflammation using the $CD45RB^{hi}$ T cell transfer model of colitis. Using a variety of criteria, including extensive phenotypic analyses and gene expression arrays, our data indicate that $F4/80^{hi}CX3CR1^{hi}$ cells are MPs that constitute the majority of the steady-state cLP mononuclear phagocytes (MNPs). These MPs can be divided into $CD11c^+$ and $CD11c^-$ populations, both of which are poor at presenting antigens to T cells, and produce large amounts of IL-10 and other antiinflammatory cytokines. In contrast, DCs express low to intermediate levels of F4/80 and CX3CR1, are $CD11c^+$, and comprise at least three separate populations: $CD103^+CX3CR1^-CD11b^-$DCs,$CD103^+CX3CR1^-CD11b^+$ DCs, but also $CD103^-CX3CR1^{int}CD11b^+$ DCs. $CD103^+$ $CX3CR1^-CD11b^-$ DCs are unique in their ability to efficiently cross-present antigens to $CD8^+$ T cells, whereas both $CD103^+CX3CR1^-CD11b^+$ DCs and $CD103^-$ $CX3CR1^{int}CD11b^+$ DCs are more efficient at presenting antigens to $CD4^+$ T cells. More importantly, we identified $Ly6C^{hi}$ MOs as precursors for the $F4/80^{hi}CX3CR1^{hi}CD11c^+$ MP population exclusively. IL-10 constitutively produced by these cells and by $CD11c^-$ MPs actively suppresses IL-12p35 and IL-23p19 production from cLP MNPs in noninflammatory conditions in vivo. In contrast, during colitis MOs differentiate into the $CD103^-CX3CR1^{int}CD11b^+$ DC population, which massively infiltrates the cLP and plays proinflammatory functions by producing IL-12, IL-23, iNOS, and TNF and driving the differentiation of IFN-γ–producing T cells. These experiments are the first to definitively identify $CX3CR1^{hi}CD11c^+$

as MPs and not DCs and to demonstrate the dual capacity of Ly6C^{hi} MOs to differentiate into regulatory or inflammatory populations depending on the local environmental conditions.

RESULTS

The steady-state cLP contains two major subsets of MPs

To characterize the phenotype of cLP MP and DC populations, we used a combination of CD45, MHC-II, lineage markers (lin: CD3, CD19, TCR-β, TCR-γδ), CD11c, and F4/80. After pregating on CD45$^+$ cells to exclude any contaminating IECs, total cLP MNPs, gated as MHC-II^{hi}lin$^-$ cells, could be subgrouped into four populations based on CD11c and F4/80 expression (Fig. 1, A and C). Two classical CD11c$^-$F4/80^{hi} MP and CD11c^{hi}F4/80$^-$ DC populations represented 39.02 ± 6.19% and 3.51 ± 1.24% of total MNPs, respectively. Interestingly, the cLP also contained a large population of cells coexpressing high levels of CD11c and F4/80 (30.83 ± 5.71%). Finally, a population of CD11c$^+$ cells with intermediate levels of F4/80 expression (10.01 ± 2.59%) could also be identified (Fig. 1, A and C). For better clarity, the four described cLP MP/DC populations will be hereafter referred to as subsets 1, 2, 3, and 4 as illustrated in Fig. 1 A. Electron microscopy revealed that both subsets 1 and 2 exhibited classical morphological and ultrastructural characteristics of MPs such as numerous phagocytic vacuoles, eccentric nuclei, and primary and secondary lysosomal granules (Fig. 1 D). In contrast, subset 4 was of smaller size and had more typical DC morphology, with less cytoplasm, cell surface dendritic projections, and lack of large intracytoplasmic vesicles. Finally, subset 3 exhibited characteristics more similar to DCs than MPs, as is shown in Fig. 1 D. Further analysis of CX3CR1, CD103, and CD11b expression on these four subsets revealed that MP subsets 1 and 2 are homogeneously CX3CR1^{hi}CD11b$^+$CD103$^-$, whereas DC subset 4 is homogeneously CX3CR1$^-$CD11b$^-$CD103$^+$. In contrast, subset 3 expresses low to intermediate levels of CX3CR1 and contains at least two separate populations of CX3CR1$^-$ CD11b$^+$CD103$^+$ (CD103$^+$ subset 3) and CX3CR1^{int} CD11b$^+$CD103$^-$ (CD103$^-$ subset 3) cells (Fig. 1 B). A more extensive flow cytometry phenotypic analysis revealed that subsets 1 and 2 both expressed the classical MP marker CD14 but also differed in their expression of Mac-3, as well as the transferrin receptor CD71, the M-CSF receptor (CD115), and the T cell co-stimulatory molecule CD70 (Fig. 1 E; Atarashi et al., 2008). The DC subset 4 did not express the MP markers CD14, Mac-3, CD70, CD115, or CD71. Subset 3 exhibited a phenotype very similar to subset 4 but seemed to express some low levels of CD14. DNA microarray analysis further supported the MP identity of subsets 1 and 2, which expressed much higher levels of F4/80, CX3CR1, CD14, CD68, mannose receptor (Mrc1), MP scavenger receptor (Msr1), lysozyme (Lyz), Fc-γ receptors (Fcgr1, Fcgr2b, Fcgr3, and Fcgr4), complement receptors (C5ar1 and C3ar1), and cathepsins (Cts), compared with subsets 3 and 4 (Fig. 1 F). In addition however, using stringent statistical analysis, 21 genes were differentially expressed between subset 1 and 2, supporting the fact that these subsets are distinct (Fig. 1 G). For example, the scavenger receptor CD163 and the coagulation factor XIII A1 polypeptide (FXIIIa1) were 12.2 ± 2.96– and 10.89 ± 3.18–fold higher in subset 1 versus 2. Furthermore, in vivo BrdU incorporation experiments were also consistent with subsets 1 and 2 being MPs, as they both exhibited much slower turnover rates, compared with DC subsets 3 and 4 (Fig. S1).

We next investigated the functional properties of colonic MPs and DCs. First, their capacity to internalize fluorescent microbeads was assessed, as a measure of their phagocytic activity. A higher percentage of subsets 1 and 2 phagocytosed beads, and these cells were more likely to contain multiple beads compared with subsets 3 and 4 (Fig. 2, A and B). Colonic subsets 1 and 2 also exhibited very low T cell priming capacities, similar to splenic MPs, and lower than subsets 3 and 4 or splenic DCs in both allogeneic (Fig. 2 C) and antigen-specific T cell proliferation assays using OT-I and OT-II TCR transgenic T cells (Fig. 2, D and E). Of note, subset 4 was less efficient at OT-II T cell priming but more efficient at OT-I T cell priming, compared with subset 3 or splenic DCs, suggesting its superior ability to cross-present antigens. Surprisingly, no striking difference in the expression of MHC-II or of the co-stimulatory molecules CD80, CD86, PD-L1, or PD-L2 could be detected between the different subsets (Fig. S2 A). However, subsets 3 and 4 were uniquely able to strongly up-regulate CCR7 expression 24 h after in vitro stimulation with LPS, suggesting their potential selective ability to migrate to the MLNs to prime T cells (Fig. S2 B).

We also sought to determine the location of the MNP populations within the colon. Immunofluorescence staining of frozen colon sections revealed that F4/80$^+$CD11c$^-$ cells (subset 1, green staining) were scattered throughout the LP, whereas F4/80$^+$CD11c$^+$ cells (subsets 2 and 3, orange staining) were located in closer proximity to the colonic epithelium (Fig. 2 F). CD11b/CD11c double staining confirmed the preferential subepithelial localization of subsets 2 and 3 (CD11b$^+$CD11c$^+$, orange staining) compared with subset 1 (CD11b$^+$CD11c$^-$, green staining; Fig. 2 F). In contrast, subset 4 (CD11c$^+$F4/80$^-$CD11b$^-$ red staining) was concentrated in lymphoid aggregates, although some of these cells could be detected occasionally in the LP (Fig. 2 F and Fig. S3).

Together, these data indicate that the steady-state cLP contains two MP and three DC populations with unique phenotypic, functional, and anatomical characteristics. Furthermore, these findings underline the fact that CD11c integrin expression, even when combined with high levels of expression of MHC-II, is not a sufficient criterion to define DCs in the cLP and identify F4/80^{hi}CX3CR1^{hi}CD11c$^+$CD11b$^+$CD103$^-$ subset 2 as a major MP subset in the cLP.

LPS induces an antiinflammatory cytokine signature in colonic MP subsets 1 and 2

We next focused on the function of the colonic MP subsets 1 and 2 in the steady-state in vivo and performed a gene expression analysis by real-time RT-PCR on FACS-purified unstimulated cells. Subsets 1 and 2 both expressed 80–100-fold

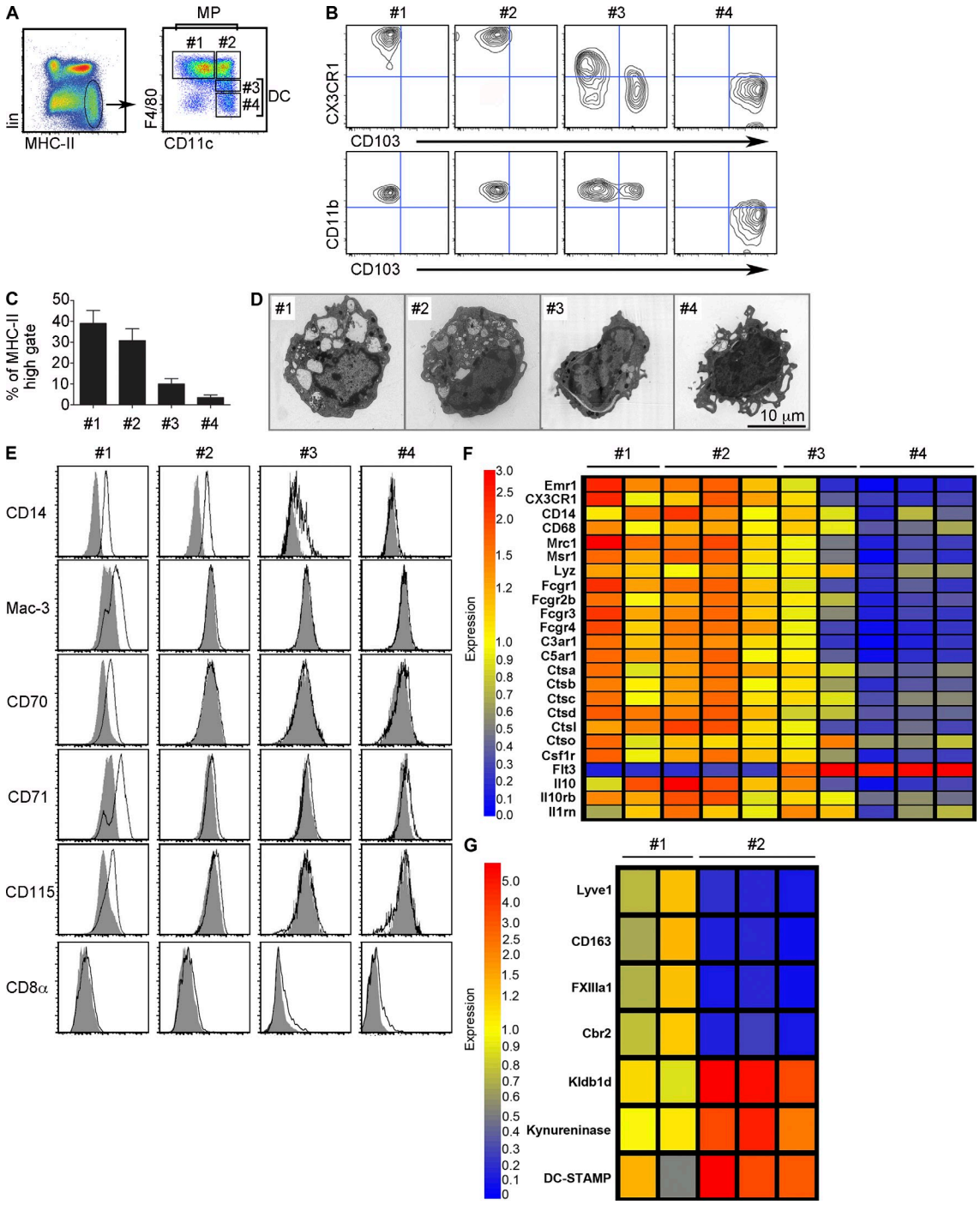

Figure 1. Definition and characterization of four DC/MP subsets in the steady-state colon. (A) Representative FACS analysis showing the gating strategy to define colonic MP and DC subsets. After pregating on CD45$^+$MHC-II^{hi}lin$^-$ cells, cLP cells were subdivided into four different populations (MP subsets 1 and 2 and DC subsets 3 and 4) based on their CD11c and F4/80 expression. (B) CX3CR1/CD103 and CD11b/CD103 expression profiles on the four MP and DC populations defined in A. Plots are representative of >20 experiments with 3–10 pooled mouse colons. (C) Quantification of the four cLP MP/DC populations (defined in A), expressed as percentages of total MHC-II^{hi}lin$^-$ cells. Data are mean ± SEM of three independent experiments with at least three pooled mouse colons. (D) Electron micrographs of cLP subsets 1–4 FACS sorted from 10 pooled mouse colons. (E) Surface phenotype of subsets 1–4. Specific markers (black lines) and isotype controls (gray-filled areas) are shown. Plots are representative of at least three independent experiments with 3–10 pooled colons each. (F) Microarray analyses of the genes differentially expressed in subsets 1–4. (H) Microarray analyses of the genes differentially expressed in subset 1 versus 2. Each replicate represents data obtained for one subset FACS sorted from 10 pooled colons.

higher messenger RNA (mRNA) levels the antiinflammatory cytokine, IL-10, relative to subset 4 (Fig. 3 A), confirming our findings from DNA microarray analysis (Fig. 1 F). Accordingly, subset 2, and to some extent subset 1, spontaneously released IL-10 after overnight culture in the absence of stimulation (Fig. 3 B). FACS analyses on colonic MNPs from IL-10–Vert-X reporter mice confirmed the high IL-10 expression levels in subsets 1 and 2 but not subsets 3 and 4 (Fig. 3, C and D). Subset 2 also expressed higher levels of TNF and iNOS mRNA (Fig. 3 E). No statistically significant

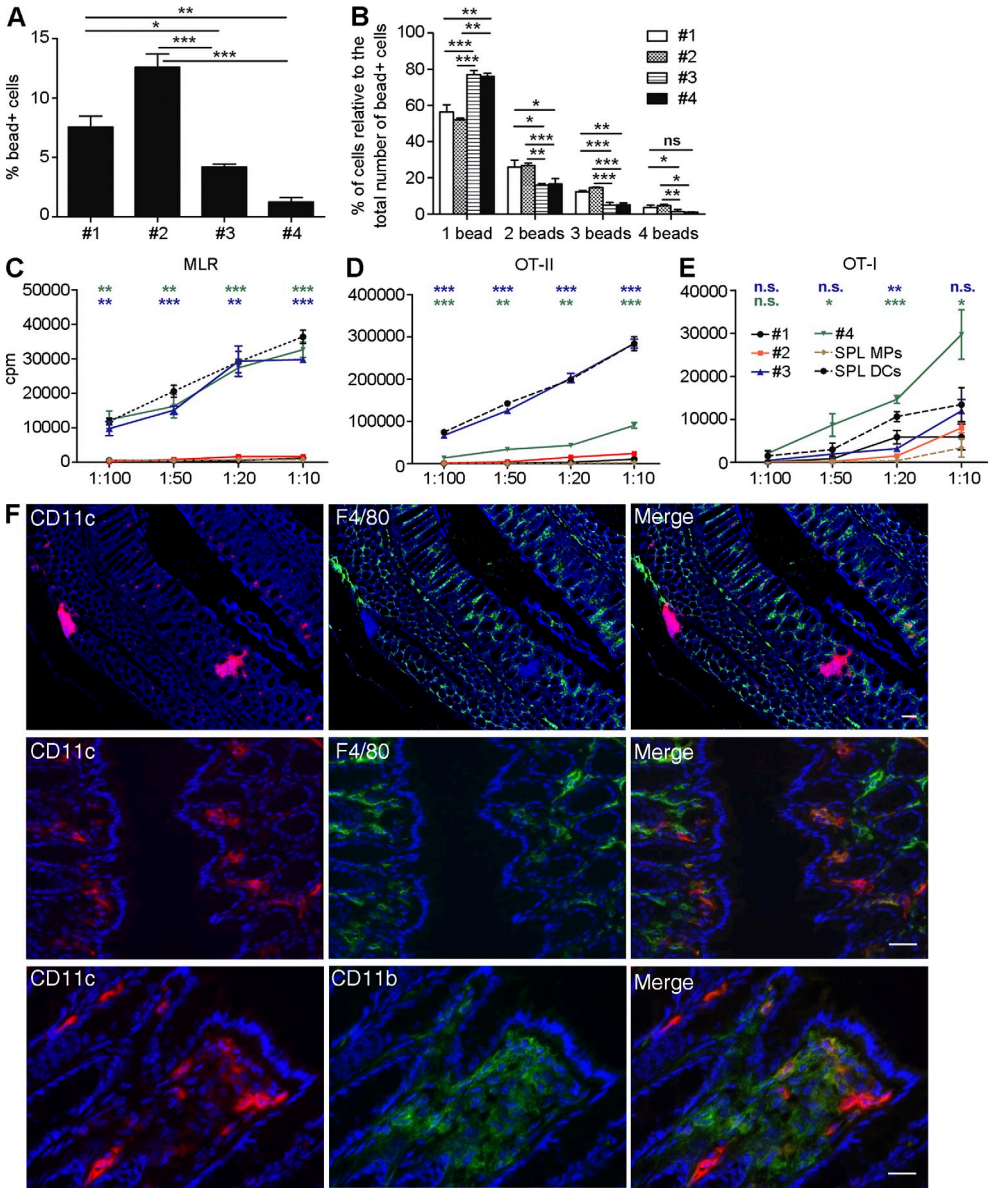

Figure 2. Functional characterization and localization of cLP MP/DC subsets and T cell priming capacities of subsets 1–4. (A and B) Phagocytic capacities of subsets 1–4. cLP cells from C57BL/6 mice were incubated in the presence of fluorescent microbeads for 45 min and analyzed for their bead content. (A) Percentage of each subset containing at least one bead. (B) Percentage of each subset containing one bead, two beads, three beads, four beads, or more after pregating on total bead$^+$ cells. Results are mean ± SD and are representative of two independent experiments with three mice each. (C) Allo-stimulatory capacities of C57BL/6 cLP subsets 1–4 and control splenic DCs and MPs co-cultured with CD4$^+$ T cells from the spleen of BALB/c at the indicated ratios. (D and E) Proliferation of OT-II (D) and OT-I (E) cells after co-culture with graded doses of OVA protein–pulsed cLP subsets 1–4 and control splenic (SPL) DCs and MPs. Proliferation was determined by thymidine incorporation assay after 4 d (C and D) or 3 d (E) of culture. Results are expressed as mean ± SD of cpm triplicates and are representative of at least two independent experiments using pooled cells from 10 mice per experiment. Unpaired Student's *t* tests were performed to compare subset 2 versus 3 (blue statistics) and subset 2 versus 4 (green). The comparison of subset 2 versus 1 never reached statistical significance. *, $P < 0.05$; **, $P < 0.01$; ***, $P < 0.001$. (F) In situ expression of CD11c (red) and F4/80 (green; top and middle) or CD11c (red) and CD11b (green; bottom) on C57BL/6 mouse colon sections. Hoechst counterstain is blue. Three mice were analyzed in three separate experiments. Bars, 50 µm.

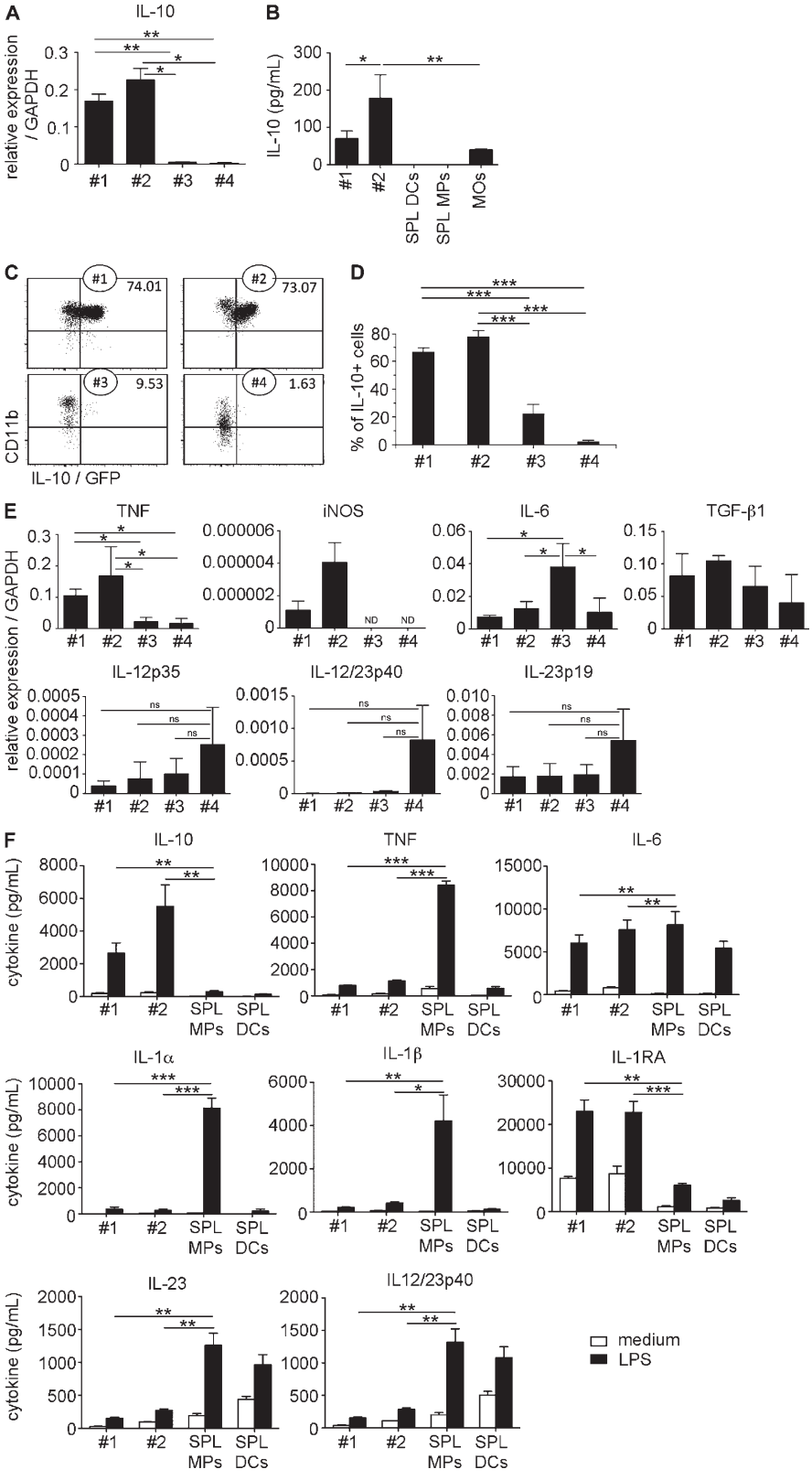

Figure 3. Subsets 1 and 2 spontaneously release the antiinflammatory cytokine IL-10 and respond to LPS stimulation with an antiinflammatory signature. (A) Real-time RT-PCR analysis of IL-10 mRNA expression by freshly isolated FACS-sorted cLP subsets from C57BL/6 mice. Results are mean real amounts ± SD, normalized to GAPDH ($1/2^{\Delta Ct}$), of at least three independent experiments with 10 pooled mice in each. (B) Spontaneous release of IL-10 measured by ELISA after overnight culture of freshly isolated FACS-sorted colonic subset 1 or 2, compared with splenic (SPL) DCs, splenic MPs, or MOs. Results are mean ± SD of three experiments with 5–10 pooled mice in each. (C and D) Representative plots (C) and quantification (D) of IL-10–GFP reporter expression by cLP subsets 1–4 freshly isolated from Vert-X mice. FACS plots present the IL-10–GFP/CD11b staining profile after pregating on each individual cLP subset. Quadrant gates were set using isotype controls. For IL-10–GFP negative controls, cells were prepared from WT mice. Results are mean ± SD of three mice analyzed separately and are representative of two experiments. (E) Real-time RT-PCR analysis of cytokine mRNA expression in FACS-sorted cLP DC/MP from C57BL/6 mice. Results are represented as real amounts, normalized to GAPDH ($1/2^{\Delta Ct}$). Data are mean ± SEM of at least three independent sorting experiments performed in duplicate. ND, not detected. (F) Quantification of the cytokines secreted by cLP subsets 1 and 2 and control splenic MPs and DCs after 24 h of culture in media alone (open bars) or in the presence of 1 µg/ml LPS (closed bars), using the SearchLight multiplex cytokine immunoassays. Results are mean ± SD of three independent experiments with 10 pooled colons and 3 pooled spleens each. *, $P < 0.05$; **, $P < 0.01$; ***, $P < 0.001$.

differences in the levels of mRNA for IL-12p35, IL-12/23p40, IL-23p19, or TGF-β1 -β2, or -β3 (Fig. 3 E and not depicted) were found between the different cLP subsets. Interestingly, consistently higher levels of IL-6 mRNA were detected in subset 3.

Because colonic MPs constitutively released IL-10, a well-known antiinflammatory cytokine, we extended this finding by measuring the pro- and antiinflammatory cytokines produced by these cells after restimulation with LPS and compared their response to the response of splenic MPs and DCs. LPS induced a massive production of IL-10 but also of IL-1 receptor antagonist (IL-1RA) by colonic MPs, whereas splenic DCs and MPs produced much lower levels of these mediators (Fig. 3 F). In contrast, colonic MPs secreted very low levels of the proinflammatory cytokines TNF, IL-1α, IL-1β, IL-23, and IL-12/23p40 compared with splenic MPs (Fig. 3 F), suggesting

that LPS induces an antiinflammatory response in subsets 1 and 2. Thus, cLP subsets 1 and 2 both spontaneously release IL-10, and LPS stimulation induces an antiinflammatory cytokine signature in these cells.

IL-10 production by cLP subsets 1 and 2 is partially dependent on the presence of commensal bacteria and regulates the production of proinflammatory cytokines by cLP DC/MP subsets

We next searched for factors that drive the production of IL-10 by colonic MPs. To examine the contribution of intestinal bacteria, we compared the IL-10 mRNA levels in colonic MPs isolated from WT mice bred in germ-free (GF) conditions versus control specific pathogen–free (SPF) mice. Importantly, the presence of intestinal bacteria did not alter the number of cells from subsets 1–4 in the colon (Fig. 4 A). However, cLP subsets 1 and 2 from GF mice showed a consistent twofold reduction in IL-10 mRNA expression compared with SPF mice (Fig. 4 B). Interestingly, IL-10 mRNA expression in cLP subsets 1 and 2 was MyD88$^{-/-}$ independent (Fig. 4 B). Collectively, these results suggest that the production of IL-10 by cLP subsets 1 and 2 in vivo is MyD88 independent and only partially driven by commensal bacteria.

We next hypothesized that IL-10 constitutively expressed by cLP MPs acts to condition surrounding cells. To investigate this, we FACS-sorted the cLP DC/MP subsets from young IL-10$^{-/-}$ mice before they developed any signs of colitis and analyzed their IL-12p35, IL-23p19, and IL-6 mRNA expression by real-time PCR, compared with WT cLP subsets (Fig. 4 C). Both IL-12p35 and IL-23p19 mRNA levels were significantly higher in cLP subsets 1–3 isolated from IL-10$^{-/-}$ mice compared with WT mice, which is consistent with the possibility that IL-10 regulates IL-12 and IL-23 production in the colon by acting in both an autocrine and paracrine manner under noninflammatory conditions. In contrast, in the absence of IL-10, the levels of IL-12 and IL-23 did not change in subset 4 (Fig. 4 C), which is physically isolated within isolated lymphoid follicles. Surprisingly, the levels of IL-6 in the cLP DC/MP subsets were either decreased or remained unchanged in the absence of IL-10. Together, these data indicate that cLP subsets 1 and 2 produce IL-10 in an MyD88-independent manner in response to commensal bacteria and other unidentified signals and that this cytokine controls the production of IL-12p35 and IL-23p19 by LP DC and MP populations.

MOs generate mostly cLP subset 2 in noninflammatory conditions

MOs have been shown to generate CX3CR1^{+}CD11b^{+}CD103^{-} LP cells in the SI (Bogunovic et al., 2009; Varol et al., 2009). We thus sought to determine whether MOs could generate CX3CR1^{+} cells (subsets 1–3) in the colon. We FACS sorted CD115^{+}Ly6C^{hi}CD11b^{hi} (Ly6C^{hi}) MOs from the bone marrow of congenic (CD45.1^{+}) mice and adoptively transferred them into recipient steady-state mice (Fig. 5, A and B). Importantly, MOs were CD11c^{-}c-kit^{-}CD11b^{hi}Flt3^{lo}MHC-II$^{lo/-}$CD11b^{hi} and were thus different from the recently described pre-DCs (Liu et al., 2009), pro-DCs (Naik et al., 2007), MP and DC precursors (Fogg et al., 2006), or the common DC precursor (Naik et al., 2007; Fig. 5 C). Additional phenotypic markers of purified MOs are depicted in Fig. S4 A. In agreement with previous studies (Geissmann et al., 2003; Bogunovic et al., 2009), we were unable to detect any MO-derived DCs or MPs in the colon of WT mice 3, 7, or 21 d after the i.v. injection of up to 3 million FACS-sorted MOs (not depicted). This is most likely because of the low proliferation potential of MOs, combined with their low rate of recruitment to the cLP (Varol et al., 2009). We thus transferred MOs into CD11c diphtheria toxin (DTx) receptor (DTR; CD11cDTR) bone marrow chimeric mice treated with DTx (Fig. 5 D; Jung et al., 2002). As illustrated in Fig. S4 (B and C), cLP CD11c^{+} DC/MP subsets were significantly decreased in the chimeras 24 h after a single injection of DTx. Interestingly, DTx treatment also depleted subset 1, which lacks significant CD11c expression. This could

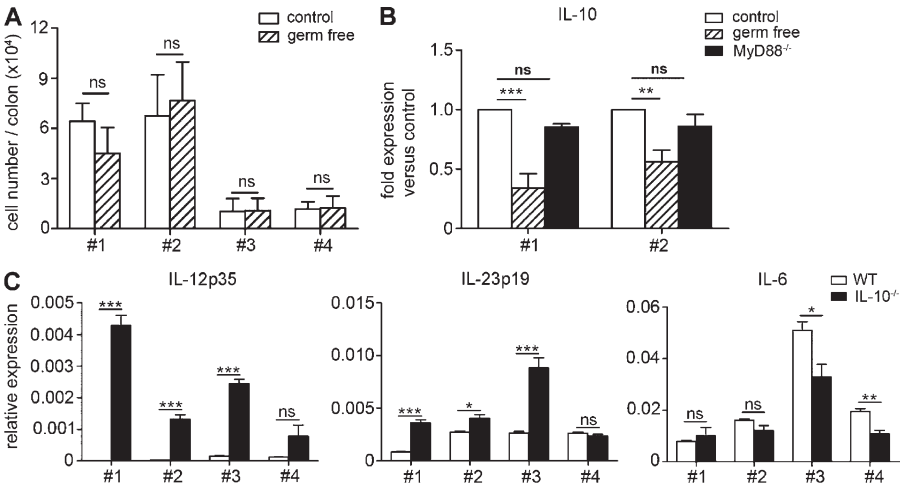

Figure 4. IL-10 production by cLP subsets 1 and 2 is partially dependent on the presence of commensal bacteria and regulates the production of proinflammatory cytokines by cLP DC/MP subsets. (A) Absolute numbers of cLP subsets 1–4 in WT and GF mice. (B) Real-time RT-PCR analysis of IL-10 mRNA expression by cLP subsets 1 and 2 FACS sorted from GF, MyD88$^{-/-}$, or WT mice. Results are mean ± SD of real amounts normalized to GAPDH ($1/2^{\Delta Ct}$) and are representative of at least two experiments with five mice each. (C) Real-time RT-PCR analysis of IL-12p35, IL-23p19, and IL-6 mRNA expression in cLP subsets 1–4, FACS-sorted WT (open bars), or IL-10$^{-/-}$ mice (closed bars) at 6 wk of age. Results are mean ± SD of real amounts normalized to GAPDH ($1/2^{\Delta Ct}$) and are representative of two experiments with 10 mice each. *, $P < 0.05$; **, $P < 0.01$; ***, $P < 0.001$. Results are mean ± SD of three experiments with three to five pooled colons per group.

result from the phagocytosis by subset 1 of dying CD11c$^+$ cells that had taken up DTx, which is an indirect consequence of the depletion of the other cLP DC/MP subsets or ectopic expression of the CD11cDTR transgene by subset 1, as has been suggested for other MP populations in this model (Probst et al., 2005; Bar-On and Jung, 2010). Importantly, the DTx treatment and DC/MP depletion did not appear to induce any significant inflammation in the cLP, as indicated by the comparable IL-1β, IL-6, TNF, IL-12p35, IL-23p19, and IL-12/23p40 mRNA expression levels in the colons of CD11cDTR chimeras injected with DTx or PBS (Fig. S4 D).

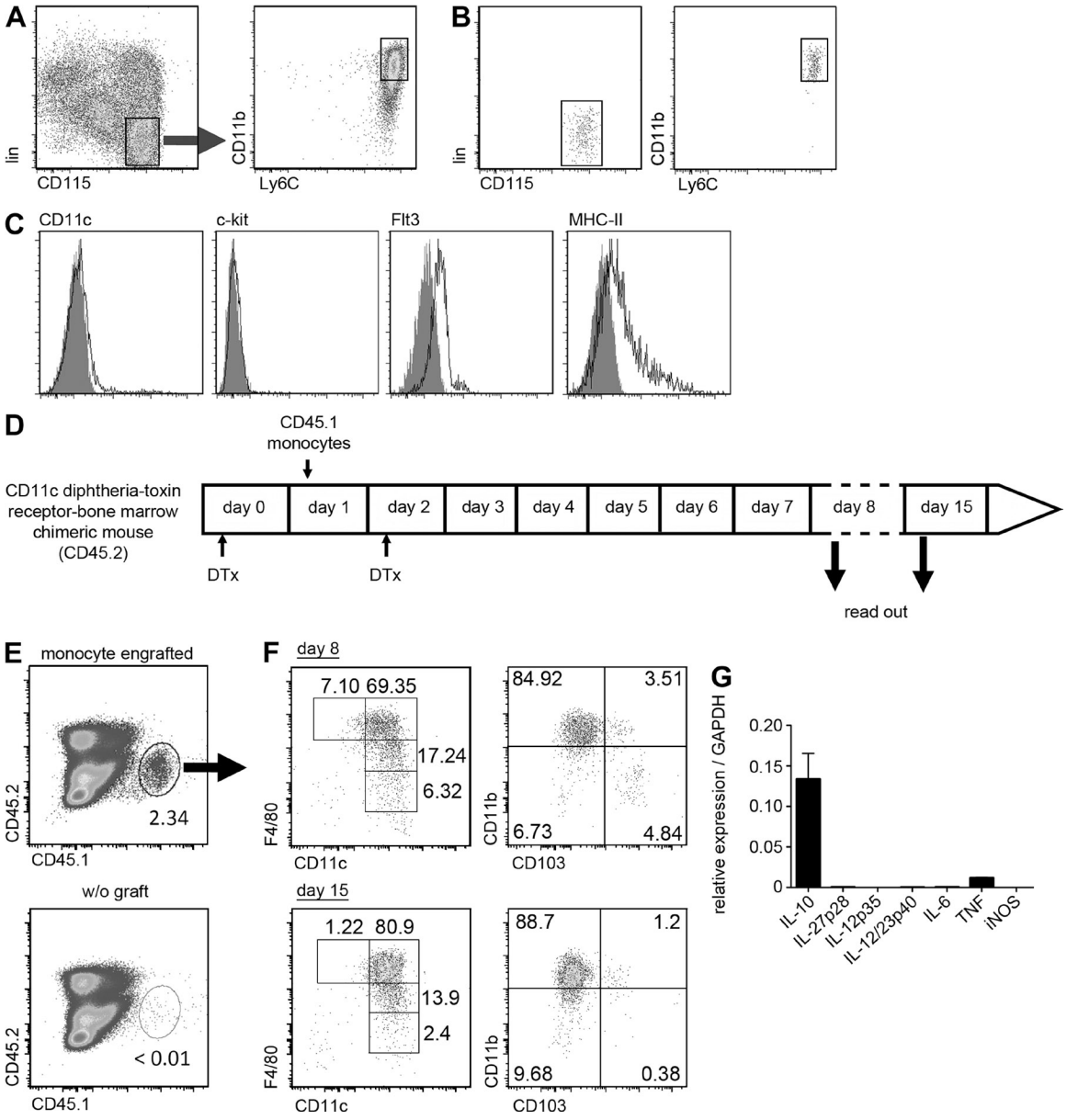

Figure 5. MOs generate mostly the immunoregulatory cLP subset 2 after adoptive transfer into CD11cDTR → C57BL/6 bone marrow chimera. (A) FACS strategy for the sorting of CD115$^+$lin$^-$ (CD3, CD4, CD8α, NK1.1, B220, CD11c, CD117 [c-kit]) Ly6C^{hi}CD11b$^+$ bone marrow of MOs. (B) Postsorting flow cytometry plots. Data are representative of at least four experiments with 10 pooled bone marrows. (C) FACS analysis of the sorted MO surface phenotype. Plots are representative of three independent experiments with 10 pooled bone marrows. (D) Schematic diagram depicting the strategy and time points used for the depletion of CD11c$^+$ cells in CD11cDTR → C57BL/6 bone marrow chimeric mice, the adoptive transfer of purified CD45.1$^+$ MOs, and the analysis of MO progeny in the colon. (E and F) FACS analysis of colonic cells from recipient CD11cDTR → C57BL/6 chimera at day 8 and 15 after i.v. graft of 2–3 × 10^6 purified CD45.1$^+$ bone marrow MOs. A nongrafted chimera is shown as a negative control (w/o graft). Data are representative of at least two separate experiments with three MO-grafted mice and controls. (G) Real-time RT-PCR analysis of cytokine mRNA expression in CD45.1$^+$ (MO derived) colonic cells FACS sorted from CD11cDTR → C57BL/6 chimera 7 d after MO graft. Results are mean real amounts ($1/2^{\Delta Ct}$) ± SD, have been normalized to GAPDH, and are representative of two experiments with five to six MO-transferred mice each.

7 d after Gr-1^{hi} MO transfer, MO-derived cells represented 2–3% of total colon hematopoietic cells (Fig. 5 E) and primarily acquired the phenotype of subset 2 (Fig. 5 F, top). However, we could not exclude the possibility that MOs also gave rise to limited numbers of DCs, as 8–10% of MO-derived cells consistently exhibited a phenotype comparable with subsets 3 and 4. Interestingly, MO-derived cells were still detectable 2 wk after transfer, and their phenotype remained largely confined to subset 2 (Fig. 5 F, bottom). Similar results were observed in the SI LP (not depicted). Finally, even though cLP MP subset 1 was depleted by the DTx treatment, MOs failed to give rise to this subset for up to 15 d after transfer (Fig. 5 F), a time at which >30% of cells of this subset had turned over (taken up BrdU) in untreated WT mice (Fig. S1).

Consistent with their subset 2 surface phenotype, FACS-sorted cLP MO-derived (CD45.1$^+$) cells expressed high levels of IL-10 and TNF but low levels of other proinflammatory cytokine mRNA (Fig. 5 G). Together, these data indicate that Ly6C^{hi} MOs selectively give rise to the cLP MP subset 2 and not subset 1 in the noninflamed colon.

MOs generate an inflammatory CD103$^-$ DC subset 3 after adoptive transfer into RAG$^{-/-}$ colitic mice

We next used the adoptive transfer model of colitis (Powrie et al., 1993) to investigate the changes in cLP MP/DC populations during chronic intestinal inflammation and to determine which cLP populations were derived from MOs under these conditions. RAG$^{-/-}$ mice adoptively transferred with naive CD45RB^{hi}CD4$^+$ T cells developed severe intestinal inflammation within 7–8 wk after transfer, as indicated by the four- to fivefold increase in the total number of hematopoietic cells (CD45$^+$) and MHC-II^{hi} MPs/DCs in the colon (Fig. 6, A and B), as well as by histological scoring (not depicted). In contrast, control RAG$^{-/-}$ mice that received a mixture of CD45RB^{hi+lo} T cells (containing T reg cells) did not develop intestinal inflammation during the same time course (Fig. 6 B; Read et al., 2000). A selective increase in the percentage of subset 3 was observed in the inflamed cLP of CD45RB^{hi}- versus CD45RB^{hi+lo}-transferred mice, whereas the percentages of subsets 1, 2, and 4 were decreased (Fig. 6, C and D). In colitic mice, subset 3 outnumbered subset 2 by two- to threefold. Interestingly, this accumulating subset 3 from CD45RB^{hi} colitic mice was almost exclusively CD103$^-$ compared with control CD45RB^{hi+lo} mice (Fig. 6, D and E), suggesting that most cells in subset 3 either down-regulated CD103 expression during colitis or were derived from newly recruited precursors that differentiated into a CD103$^-$ subset 3 in the colitic environment. In support of the latter possibility, the CD103$^-$ subset 3 expressed E-cadherin, a marker previously shown to be expressed on inflammatory DCs recruited to the colon of colitic mice (Fig. S5 A; Siddiqui et al., 2010), as well as the monocytic lineage marker CX3CR1 (Fig. S5 B). Moreover, Ly6C^{hi} MOs adoptively transferred into colitic mice rapidly migrated to the inflamed colon (Fig. 6 F) and largely developed into cells that were phenotypically similar to the endogenous CD103$^-$ subset 3 that massively infiltrated the cLP (Fig. 6 G). Additionally, a larger proportion of the MO-derived cells in the colitis environment corresponded to subset 3 and possibly 4, compared with what was observed in the adoptive transfer experiments in noninflamed mice (20–25% vs. <10%, respectively). Gene expression profiling of MO-derived cells sorted from colitic recipient animals showed that mRNAs for all inflammatory cytokine (IL-12p35, IL-12/23p40, IL-23p19, IL-6, and TNF) were up-regulated compared with MO-derived cells sorted from noncolitic mice, whereas the levels of IL-10 mRNA from MO-derived cells from colitic mice were decreased (Fig. 6 H).

Together, these data suggest that a proinflammatory CD103$^-$ subset 3 producing IL-12, IL-23, IL-6, TNF, and iNOS dramatically accumulates in the cLP from colitic mice, whereas the CD103$^+$ fraction of subset 3 decreases dramatically. This infiltrating inflammatory CD103$^-$ subset 3 is derived from circulating Ly6C^{hi} MOs whose differentiation potential is changed when recruited to the inflamed cLP, compared with the noninflamed cLP. Finally, our data suggest that Ly6C^{hi} MOs also give rise to a much smaller proportion of MP subset 2, as well as to CD103$^+$ populations during colitis (Fig. 6 G).

CD103$^-$ subset 3 exhibits potent T cell priming capacities and induces the differentiation of IFN-γ–producing T cells in vitro

The MO-derived CD103$^-$ subset 3 is also present in the noninflamed cLP, although it is largely outnumbered by MO-derived subset 2 (Figs. 1 B and 5 F). Our finding that the CD103$^-$ subset 3 exhibits inflammatory functions during colitis led us to investigate the specific properties of this population under normal homeostatic conditions. In OT-II T cell priming assays, CD103$^-$ subset 3 sorted from WT mice was as efficient as CD103$^+$ subset 3 and splenic DCs and slightly more efficient than subset 4 in stimulating T cell proliferation (Fig. 7 A). Surprisingly, CD103$^-$ subset 3 FACS sorted from WT mice and pulsed with OVA protein induced the most potent differentiation of IFN-γ–producing OT-II cells compared with CD103$^+$ DC subset 3 and DC subset 4 (Fig. 7, B–D), whereas MP subsets 1 and 2 did not induce any significant IFN-γ production by T cells. In contrast, CD103$^+$ subset 3 uniquely induced the conversion of Foxp3$^+$ T reg cells from naive OT-II T cells (Fig. 7, B and C), and this finding was further supported by the higher expression level of aldh1a2 in this subset (not depicted; Denning et al., 2011). Of note, both MP subsets 1 and 2 became strong foxp3$^+$ T reg cell inducers in the presence of exogenous recombinant TGF-β (not depicted), as previously documented for SI LP MPs (Denning et al., 2007b). In addition, both CD103$^+$ and CD103$^-$ subset 3 induced low levels of IL-17 production by OT-II cells (Fig. 7 B). However, these levels didn't reach statistical significance when measured by ELISA (Fig. 7 D). Importantly, BrdU incorporation experiments showed that CD103$^-$ subset 3 had a turnover rate similar to CD103$^+$ subset 3 or subset 4 and therefore is unlikely to arise from subsets 1 or 2, which have a much slower turnover

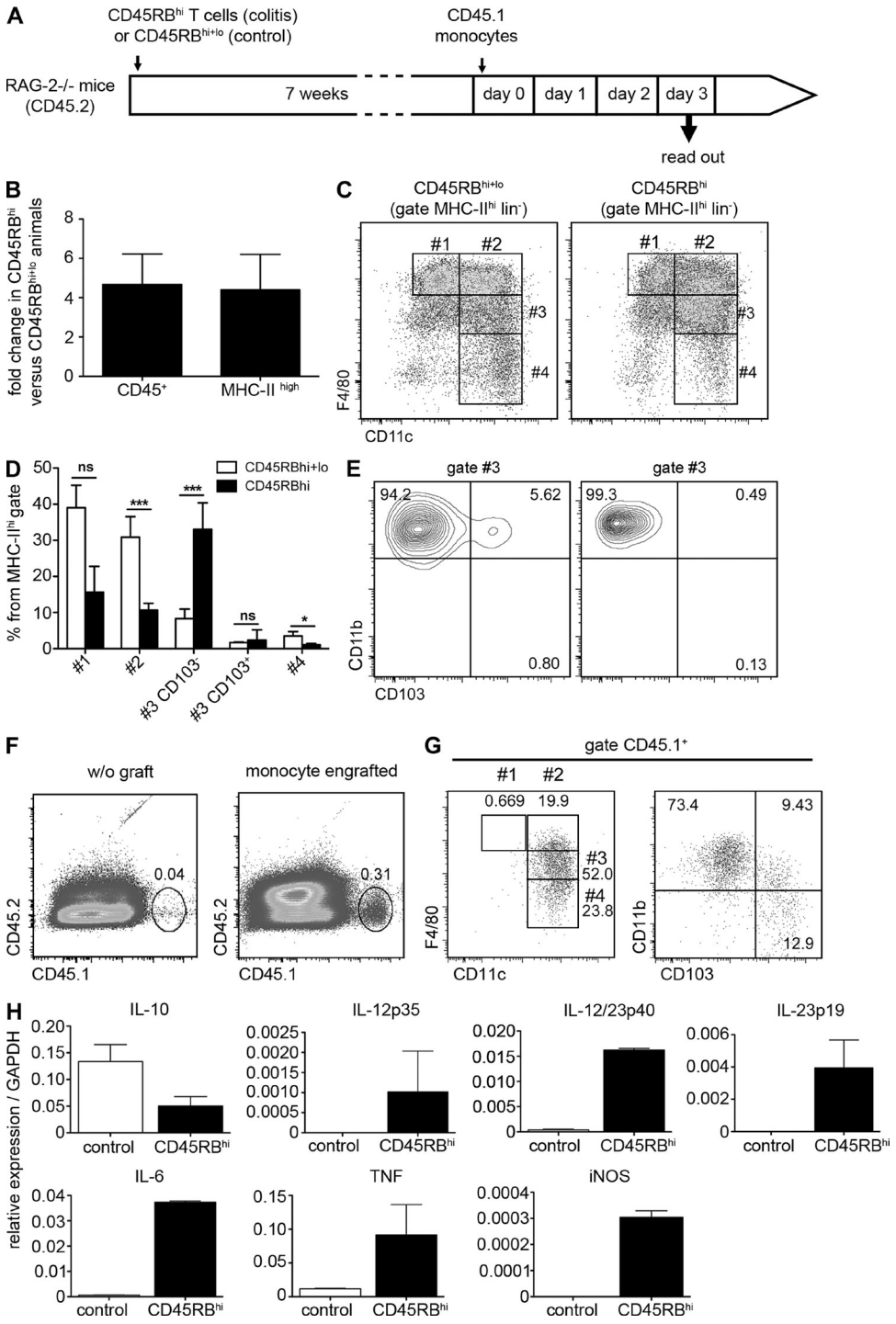

Figure 6. MOs generate an inflammatory CD103⁻ DC subset 3 after adoptive transfer into RAG$^{-/-}$ colitic mice. (A) Strategy used for the induction of colitis in Rag$^{-/-}$ mice, the adoptive transfer of purified MOs, and the analysis of MO progeny in the colon. (B) Quantification of the total number of colonic CD45$^+$ and MHC-II^{hi} cells expressed as fold change in CD45RB^{hi} (colitic) versus CD45RB^{hi+lo} (control) animals. Results are mean ± SD of three independent experiments with at least five mice per group. (C and D) Representative FACS plots (C) and quantification (D) of subsets 1, 2, 3 CD103$^-$, 3 CD103$^+$, and 4 in the colon of colitic versus control mice 7 wk after transfer of CD45RB^{hi} or CD45RB^{hi+lo} CD4$^+$ T cells, respectively. Results are mean ± SD of three independent experiments with at least five mice per group. *, $P < 0.05$; ***, $P < 0.001$. (E) CD11b/CD103 expression on subset 3 in colitic versus control mice. (F and G) Analysis of the colon of colitic mice 3 d after engraftment or not with 2–3 × 10^6 purified bone marrow MOs. The data presented are representative of at least two separate experiments with three MO-transferred mice each. (H) Real-time RT-PCR analysis of cytokine mRNA expression in CD45.1$^+$ (MO derived) colonic cells FACS sorted from recipient colitic mice 3 d after adoptive transfer of 3 × 10^6 bone marrow MOs (closed bars). The mRNA profile of MO-derived cells sorted from noncolitic CD11cDTR → C57BL/6 chimeric mice (data duplicated from Fig. 5 G) has been plotted here for comparison purposes (open bars). Results are mean ± SD of two experiments with five to seven pooled colons/group.

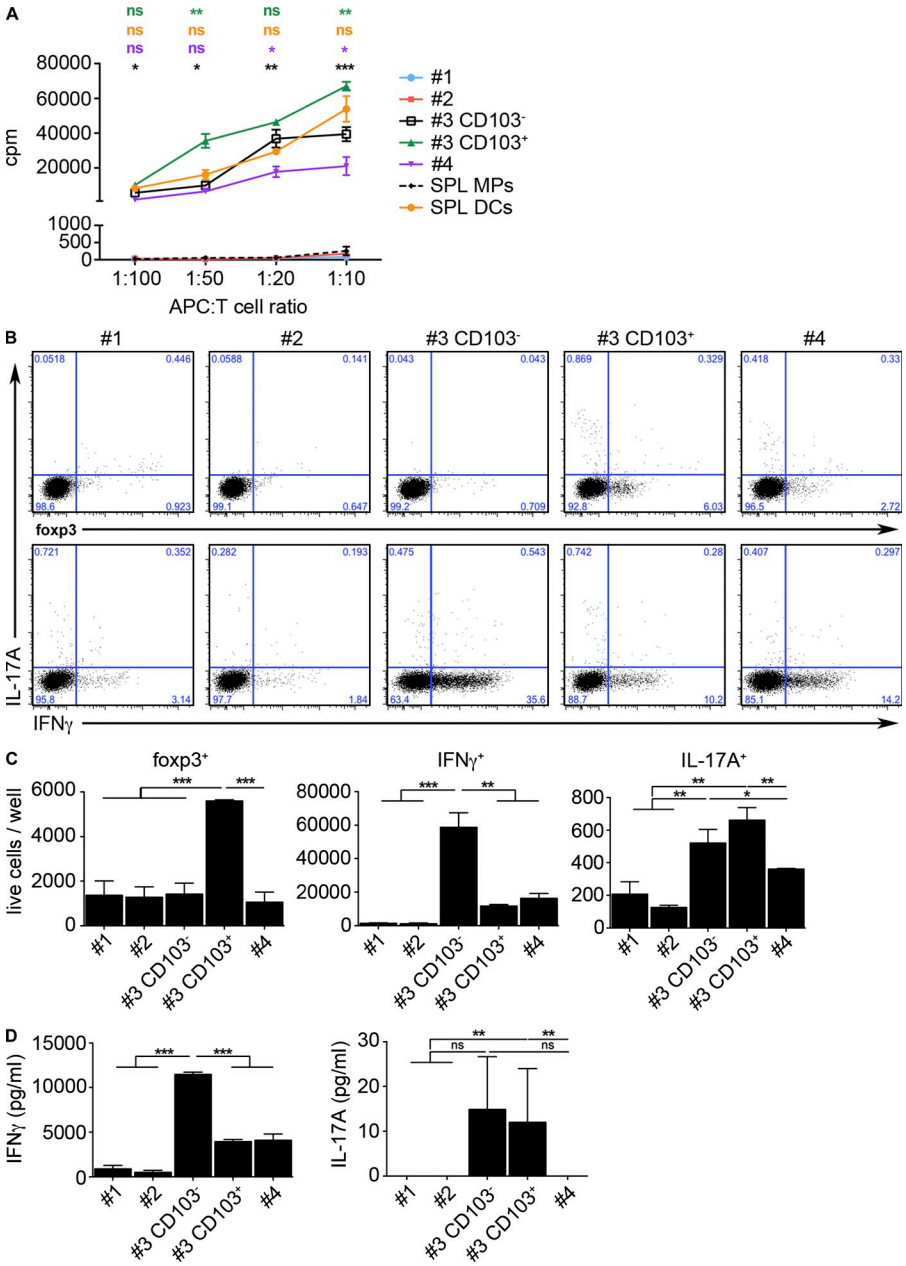

Figure 7. CD103⁻ subset 3 exhibits potent T cell priming capacities and induces the differentiation of IFN-γ–producing T cells in vitro. (A) Proliferation of OT-II cells after co-culture with graded doses of OVA protein–pulsed cLP subsets 1, 2, 3 CD103⁻, 3 CD103⁺, and 4 and control splenic (SPL) DCs and MPs. Proliferation was determined by thymidine incorporation assay after 4 d of culture. Data are mean ± SD and are representative of two experiments performed in triplicates. Subset 3 CD103⁻ was compared with subset 1 or 2 and splenic MPs using an unpaired Student's *t* test, and the less significant p-values were plotted (black statistics). Subset 3 CD103⁻ was also compared with subset 3 CD103⁺ (green statistics), subset 4 (violet statistics), and splenic DCs (orange statistics). foxp3, IFN-γ, and IL-17A intracellular FACS staining in OT-II cells co-cultured for 5 d with FACS-sorted OVA-loaded colonic subsets 1, 2, and 3 (CD103⁻ or CD103⁺) from WT mice. (B) Representative plots. (C) Quantification of the absolute numbers of live foxp3⁺, IFN-γ⁺, and IL-17A⁺ OT-II cells/well in the co-cultures. (D) Quantification of IFN-γ and IL-17A production by OT-II cells after 4.5 d of culture. (C and D) Data are mean ± SD of two separate experiments performed in triplicates. *, P < 0.05; **, P < 0.01; ***, P < 0.001.

rate (Fig. S1). Together, these data show that CD103⁻ subset 3 exhibits characteristics of inflammatory DCs even when taken from the steady-state cLP.

DISCUSSION

We comprehensively analyzed the phenotype and function of populations of MNPs in the mouse colon (Table S2), integrating markers used in prior separate studies (Denning et al., 2007b, 2011; Jaensson et al., 2008; Monteleone et al., 2008; Bogunovic et al., 2009; Schulz et al., 2009; Varol et al., 2009; Laffont et al., 2010; Niess and Adler, 2010; Platt et al., 2010; Siddiqui et al., 2010; Takada et al., 2010; Weber et al., 2011). We demonstrated that the expression of the integrin CD11c is not sufficient to distinguish DCs from MPs in the cLP. Instead, cells expressing high levels of F4/80 or CX3CR1 more clearly identified MPs based not only on their MP morphology, ultrastructural characteristics, and high phagocytic and low T cell priming capacities, but also on their transcription profiles and their lack of CCR7 expression upon activation, which suggests their inability to migrate to the draining MLNs. Consistent with our results in the colon, Schulz et al. (2009) proposed that SI LP CX3CR1⁺ cells are tissue-resident MPs, based on their low *aldh1a2* expression and aldehyde dehydrogenase activity, inability to efficiently induce the proliferation or CCR9 expression on responding T cells, and inability to migrate to the draining MLNs in the steady-state or after oral administration of the TLR7/8 ligand R848, in comparison with SI LP CD103⁺ DCs. Furthermore, Bogunovic et al. (2009) reported that the proportion of CX3CR1⁺ cells in the MLNs was not affected in CCR7$^{-/-}$ mice in comparison with the proportion of CD103⁺CD11b⁺ DCs, which is highly reduced. These observations, together with the fact that no CX3CR1^{hi} cells can be found in the MLNs, further support the notion that high expression levels of CX3CR1 or F4/80 identify tissue-resident MPs in both the SI and the colon.

Most importantly, we also revealed here that CX3CR1^{+} cells in the colon include both MPs and DCs. Indeed, in addition to CX3CR1^{hi} MPs, the majority of the MO-derived inflammatory CD103^{-} DC subset 3 also expresses intermediate levels of CX3CR1. This inflammatory DC population is present in the normal colon, but massively increases in number in the LP during colitis, and is capable of inducing naive T cells to differentiate into Th1 cells. This CX3CR1^{int}CD103^{-} DC subset 3 could represent the murine equivalent of the CD14^{+}CD68^{+}DC-SIGN^{+}CD205^{+} MPs/DCs infiltrating the LP of Crohn's disease patients (Kamada et al., 2008).

Consistent with our findings, recent studies have suggested that a balance between anti- and proinflammatory CX3CR1^{+} MNPs regulates intestinal homeostasis; however, none have clearly characterized the cell types involved. Thus, it was shown that a population of CX3CR1^{hi} MNPs that does not produce TNF in response to stimulation predominated under steady-state conditions (Platt et al., 2010; Weber et al., 2011), whereas a CX3CR1$^{lo/int}$ population of MNPs, polarized toward proinflammatory responses, infiltrated the cLP during dextran sulfate sodium–induced (Platt et al., 2010) or T cell transfer (Weber et al., 2011) colitis development. Interestingly, CX3CR1^{hi} MNPs retain their noninflammatory profile during colitis (Weber et al., 2011). We would like to propose here that the CX3CR1^{hi} intestinal MNPs described in these studies consist of the two populations of F4/80^{hi} CX3CR1^{hi} subsets clearly demonstrated to be MPs in our present work. In contrast, the CX3CR1^{lo} MNPs correspond to the proinflammatory CD11c^{+}CD11b^{+}CD103^{-} MO-derived subset of DCs (subset 3 CD103^{-}) that accumulates in the inflamed mucosa during colitis in our experiments. Siddiqui et al. (2010) also recently reported that inflammatory DCs accumulate in the colon of colitic mice and express E-cadherin. Consistent with these finding, we found E-cadherin to be expressed by the CX3CR1^{int}CD103^{-} DC subset 3 during colitis (Fig. S5 A). However, we also found this marker to be broadly induced on cLP CX3CR1^{hi} MP subsets 1 and 2.

The current experiments further demonstrate that Ly6C^{hi} MOs are precursors of both the immunoregulatory CX3CR1^{hi} MP subset 2 and the proinflammatory CX3CR1^{int}CD103^{-} DC subset 3 and that their differentiation program in the cLP is switched during inflammatory conditions from the MP subset 2 to DC CD103^{-} subset 3. The factors involved in this switch and thus controlling the balance between subset 2 and CD103^{-} subset 3 differentiation in the cLP remain to be identified but may include IL-10 and TGF-β, both of which have been shown to limit the accumulation of inflammatory DCs in tissues and favor MP differentiation (Sica et al., 2008; Guilliams et al., 2009; Siddiqui et al., 2010). There also remains the possibility that in the absence of inflammation, MOs first differentiate into the CD103^{-} DC subset 3 before becoming subset 2; however, this seems unlikely based on BrdU labeling experiments.

The MO-derived CD103^{-}CX3CR1^{int} DC subset 3 also accumulates in the MLNs of colitic mice (Guilliams et al., 2009; Varol et al., 2009; Siddiqui et al., 2010; unpublished data). Considering their proinflammatory properties, their potent T cell priming capacities, and their ability to strongly up-regulate CCR7 expression upon in vitro culture in the presence of LPS (Fig. S2), it is tempting to speculate that these cells can migrate from the cLP to the MLNs during colitis. In an intravital microscopy study, Schulz et al. (2009) were unable to detect any CX3CR1^{+} cells migrating to the MLNs in the steady-state or after oral administration of R848; however, this TLR ligand may represent an appropriate stimulus to induce the migration of CD103^{+} DCs but not CX3CR1^{int} DCs. Further work is thus necessary to clarify whether the CX3CR1^{int}CD103^{-} DC subset 3 migrates from the colon to the MLNs and/or whether blood MOs directly home to the MLNs to generate this subset, notably under chronic inflammatory conditions, as it was suggested by Cheong et al. (2010) in skin-draining LNs after LPS or gram-negative bacteria i.v. injections. This clarification is particularly important because the CX3CR1^{int}CD103^{-} DC subset 3 may overlap with the previously described CD11c^{+}CX3CR1^{+} cells, which send protrusions through the IEC layer to actively sample luminal antigens and are involved in bacterial clearance but whose potential migration to the draining MLNs is still debated (Niess et al., 2005; Vallon-Eberhard et al., 2006; Hapfelmeier et al., 2008).

The function of the CX3CR1^{hi} MP subsets 1 and 2 in the colon remains elusive. If they do not migrate out of the LP, they are unlikely to encounter naive T cells or to be involved in their priming in the MLNs. In agreement with this reasoning, we found that MP subsets 1 and 2 were very inefficient at priming T cells in vitro. However, subsets 1 and 2, via their high IL-10 production, might modulate the functions and stability of foxp3^{+} T reg cells and other effector T cells that enter the LP, subsequent to their differentiation in MLNs. Indeed, the production of IL-10 by CX3CR1^{+} cells was shown to drive the expansion of foxp3^{+} T reg cells within the LP in an oral tolerance induction protocol (Hadis et al., 2011) and to stabilize their foxp3 expression during early inflammation (Murai et al., 2009). Considering their high phagocytic capacities and their well-documented efficient uptake of bacteria, conidia from fungi, or soluble antigens (Niess et al., 2005; Vallon-Eberhard et al., 2006; Hapfelmeier et al., 2008; Bogunovic et al., 2009; Schulz et al., 2009), subsets 1 and 2 could provide essential innate immunity to preserve the intestinal barrier by phagocytosing and killing commensal bacteria that penetrate into the cLP. Indeed, these cells express high levels of phagocytic and endocytic receptors such as the MP mannose receptor (Mrc1), complement receptors C5aR and C3aR, Fc-γ receptors (Fcgr1, Fcgr2b, Fcgr3, and Fcgr4), and the MP scavenger receptors Msr1 and CD163, as well as high levels of lysozyme and multiple cathepsins (Fig. 1, F–H). Furthermore, subsets 1 and 2 likely perform this innate clearance task while constantly dampening the inflammation driven by these commensals, notably via the production of IL-10. We indeed showed here that subsets 1 and 2 produce low levels of proinflammatory cytokines compared with splenic MPs, even after LPS stimulation,

but instead constitutively release high levels of IL-10. This IL-10 controls the production of IL-12p35 and IL-23p19 by subset 3 as well as their own production of these cytokines in an autocrine manner. Several pieces of data in the literature support this notion. First, the neutralization of the IL-10 receptor on colonic CD11c$^+$ cells (>80% of which correspond to subset 2; Fig. 1 C) restores their IL-12 production to levels comparable with splenic CD11c$^+$ DCs (Monteleone et al., 2008). Second, mice with a myeloid-specific deletion of the transcription factor STAT3, both downstream of the IL-10 receptor and upstream of IL-10 production, develop a chronic enterocolitis (Takeda et al., 1999). Furthermore, colitis development in IL-10$^{-/-}$ mice results from the absence of suppression of MyD88-dependent commensal-induced inflammation by IL-10 (Rakoff-Nahoum et al., 2006). We provide evidence that commensal bacteria contribute to the production of IL-10 by cLP subsets 1 and 2, but other mechanisms are also involved, and none require MyD88 signaling.

The functions of CD11c$^+$ and CD11c$^-$ MPs may be largely redundant, as each shares phenotypic and functional characteristics, including the constitutive production of IL-10 in the cLP, and largely similar baseline gene expression. However, our data also suggest that these two MP populations have unique origins and biological functions. Thus, although both MP subsets 1 and 2 have a slow turnover rate compared with LP DC populations, only the CD11c$^+$ MP subset 2 is readily derived from MOs after cell depletion. No MO-derived subset 1 could be detected in our MO transfer experiments at day 8 or 15, a time point when the endogenous population of subset 1 was already fully reconstituted (not depicted). It is therefore unlikely that MOs are precursors of MP subset 1 or that subset 2 is an intermediate differentiation state between MOs and subset 1 under these noninflammatory conditions.

Finally, in our hands, Ly6C^{hi} MOs also appeared to give rise to at least some CD103$^+$ cells (falling into subsets 3 and 4) during colitis (Fig. 6 F). Although this finding is inconsistent with current data indicating a pre-DC origin of CD103$^+$ DCs, to our knowledge, the origin of CD103$^+$ DCs has not yet been evaluated in the presence of ongoing inflammation, nor has CD103 expression on MO-derived CX3CR1$^+$ cells. This finding is even more intriguing, considering that CD103$^+$ DCs have recently been shown to lose their tolerogenic properties during colitis (Laffont et al., 2010). Interestingly in the lungs, Jakubzick et al. (2008) documented that Ly6C^{hi} MOs preferentially repopulate CD103$^+$ DCs, whereas Ly6C^{lo} MOs repopulate CD11b^{hi} DCs, further supporting the concept that the DC/MP differentiation potential of MOs may vary depending on the organ and environment to which these precursors home.

These results are consistent with two recent articles demonstrating that MOs are precursors of MHC-II$^+$CD11c$^+$CD11b$^+$CD103$^-$CX3CR1$^+$ cells in the SI LP and cLP in steady-state conditions, whereas CD103$^+$ DCs were mostly derived from pre-DCs (Bogunovic et al., 2009; Varol et al., 2009). However, these studies did not analyze the origin of CD11c$^-$ cell populations and so did not address the differential origin of intestinal MP populations. In addition, our DNA microarray analyses further support the possibility that subsets 1 and 2 represent distinct MP populations. cLP subset 1 expresses higher levels of CD163, FXIIIa1, and Lyve1, which have been previously associated with MPs involved in wound healing or tissue repair (Philippidis et al., 2004; Schledzewski et al., 2006; Quatresooz et al., 2008). In comparison, subset 2 expresses higher levels of DC-specific transmembrane protein (DC-STAMP), which was recently shown to be involved in regulating DC functions and preventing autoimmunity development (Sawatani et al., 2008). Further work is necessary to understand the respective roles and origins of subsets 1 and 2.

In summary, our data illustrate a dual role of MOs in gut MP/DCs homeostasis. MOs may contribute to the maintenance of colon homeostasis in the steady-state by generating the cLP CX3CR1^{hi} MP subset 2, which produces regulatory cytokines, including IL-10, but may also contribute to colitis pathogenesis by generating a CX3CR1^{int}CD103$^-$ DC subset 3 that exhibits proinflammatory properties in the inflamed colon. The identification of the colonic factors controlling the differentiation of MOs into pro- or antiinflammatory MNPs and determining the mechanisms regulating IL-10 production by subsets 1 and 2 will be important steps in understanding intestinal pathophysiology and could open promising therapeutic options for patients with inflammatory bowel diseases.

MATERIALS AND METHODS

Mice

C57BL/6 and C57BL/6 SJL mice were obtained from the National Cancer Institute and used at 6–12 wk of age. C57BL/6 GF animals were bred at the National Institute of Allergy and Infectious Diseases colony from Taconic before transfer to the GF facility at the National Institutes of Health and screened weekly for viral, bacterial, and fungal contamination. Control SPF, C57BL/6 *Rag2*$^{-/-}$, C57BL/6 Rag1$^{-/-}$ OT-I, and OT-II transgenic mice were also purchased from Taconic. IL-10–GFP transcriptional reporter mice (Vert-X mice) were obtained from C. Karp (Cincinnati Children's Hospital Medical Center, Cincinnati, OH). CX3CR1$^{GFP/GFP}$, B6.129P2-IL10^{tm1Cgn}/J, and CD11cDTR mice were purchased from The Jackson Laboratory. CX3CR1$^{+/GFP}$ mice were obtained by crossing CX3CR1$^{GFP/GFP}$ with WT C57BL/6 mice. All mice were maintained at an American Association for the Accreditation of Laboratory Animal Care–accredited animal facility at the National Institute of Allergy and Infectious Diseases and housed in accordance with the procedures outlined in the Guide for the Care and Use of Laboratory Animals under an animal study proposal approved by the National Institute of Allergy and Infectious Diseases Animal Care and Use Committee.

Experimental animal models

T cell transfer colitis. *Rag2*$^{-/-}$ mice were injected i.p. with 3×10^5 CD4$^+$ CD45RB^{hi} T cells (colitic CD45RB^{hi} mice) or 1.5×10^5 CD4$^+$CD45RB^{hi} + 1.5×10^5 CD4$^+$CD45RB^{lo} T cells (noncolitic CD45RB^{hi+lo} mice) isolated from the spleens of WT mice. Mice were housed with nonsterile bedding and given nonsterile food and nonacidified water. Mice from the colitic group developed significant intestinal inflammation 7–8 wk after transfer.

CD11cDTR bone marrow chimeric mice and CD11c$^+$ cell depletion. C57BL/6 mice were irradiated (900 rads) and transferred i.p. with 3×10^6 total bone marrow cells isolated from CD11cDTR mice. CD11cDTR → C57BL/6 bone marrow chimeric mice received drinking water containing

antibiotics (0.13 mg/ml Trimethoprim and 0.67 mg/ml Sulfamethoxazole) for 6 wk. For $CD11c^+$ cell depletion, CD11cDTR → C57BL/6 bone marrow chimeric mice were injected i.p. with DTx (8 ng/g body weight; Sigma-Aldrich) as indicated.

Isolation and FACS analysis of colon and spleen phagocyte subsets. After removing extraintestinal fat tissue and blood vessels, colons were flushed of their luminal content with HBSS, opened longitudinally, cut into 2-cm pieces, and incubated with HBSS containing 0.015% DTT (15 min, 37°C in a shaking water bath). Epithelial cells and mucus were removed by extensive washes in HBSS, 5% FCS, and 25 mM Hepes before colons were cut into smaller 2-mm^2 pieces and digested in complete Iscove's media containing 167 μg/ml Liberase TL and 30 μg/ml DNase I (Roche) for 60 min at 37°C in a shaking water bath. The digested cell suspension was then passed through 100- and 40-μm cell strainers and resuspended in 1.077 g/cm^3 iso-osmotic metrizamide medium (NycoPrep; Accurate Chemical & Scientific Corp.). After centrifugation at 1,600 *g* for 15 min at room temperature, the low-density fraction was collected. For FACS analysis or sorting of colon samples, cells were stained with Fc block/anti-CD16/32 (2.4G2) and antibodies to CD11c (HL-3), MHC-II (AF6-120.1), F4/80 mAb (BM8), CD11b (M1/70), and CD103 (M290), as well as antibodies to B cell and T cell lineages (referred hereafter as lin): CD19 (RA3-6B2), CD3 (145-2C11), TCR-β (H57-597), and TCR-γδ (eBioGL3), all from eBioscience. When FACS analysis was performed directly on the digested colonic cell suspension (without NycoPrep gradient preenrichment), cells were pregated on hematopoietic cells using α-CD45.2 (104) antibody. Live/dead cells were identified using the Live/Dead Fixable violet dead cell stain kit (Invitrogen), according to the manufacturer's instructions. For the FACS-sorting of spleen MPs and DCs, lineage $(CD3/CD19/TCR\text{-}\beta/TCR\text{-}\gamma\delta)^+$ cells were first excluded. MPs were then sorted as $CD11c^-F4/80^+$ cells, whereas DCs were sorted as $CD11c^+F4/80^{-\text{ to int}}$ cells.

Other antibodies used in this paper include CD45.1 (A20), CD14 (Sa2-8), Mac3 (M3/84), CD70 (FR70), CD71 (C2), CD115 (AFS98), CCR6 (clone 140706; R&D Systems), CCR7 (4B12), CD25 (7D4), CD40 (3/23), CD69 (H1.2F3), CD80 (16-10A1), CD86 (GL-1), PD-L1 (MI-H5), PD-L2 (122), Ly6C (AL-21), c-kit (2B8), Flt3 (A2F10), E-cadherin (36), and CX3CR1 (rabbit polyclonal; Abcam), as well as corresponding isotype controls, all purchased from BD or eBioscience, unless otherwise specified. Cells were analyzed on an LSR II flow cytometer (BD) or sorted using a FACSVantage or FACSAria machine (BD).

Isolation and adoptive transfer of bone marrow MOs. 3×10^6 Fms-like tyrosine kinase 3 ligand (FLT3-L)–expressing B16 cells were injected s.c. in C57BL/6 SJL donor mice 12–14 d before MO isolation to increase their total bone marrow MO numbers. Bone marrow was flushed from the tibias and femurs of donor mice. After red blood cell lysis using ACK lysis buffer, $CD115^+$ cells were MACS enriched using an α-CD115 biotinylated antibody (eBioscience) followed by antibiotin microbeads (Miltenyi Biotech) according to the manufacturer's instructions. CD115-enriched cells were then stained for Ly6C (AL21), CD11b (M1/70), streptavidin-PE, and a mixture of lin antibodies (CD3 [145-2C11], CD4 [RM4-5], CD8 [53-6.7], CD19 [RA3-6B2], NK1.1 [PK136], CD11c [N418], and c-kit [2B8]). MOs were sorted based on $lin^-CD115^+Ly6C^{hi}CD11b^{hi}$. MO purity after sorting was consistently >98%.

Immunofluorescence staining of colonic tissue sections. Colon tissue was frozen in OCT medium (Sakura). 8-μm cryosections were fixed in acetone (30 s, −20°C) and stained with hamster anti–mouse CD11c (N418; eBioscience) and rat anti–mouse F4/80-biotin (MCA 497B; AbD Serotec) or rat anti–mouse CD11b-biotin (M1/70; eBioscience) antibodies. CD11c staining was detected using goat anti–hamster horseradish peroxidase (Jackson ImmunoResearch Laboratories, Inc.) followed by Alexa Fluor 594–tyramide (Invitrogen). After two 15-min quenching sessions in Peroxidase Blocking Reagent (Dako), F4/80 or CD11b staining was revealed by streptavidin horseradish peroxidase and Alexa Fluor 488–tyramide (Invitrogen). Slides were counterstained with Hoechst nuclear stain (Sigma-Aldrich), mounted with Fluoromount-G medium (SouthernBiotech), and visualized using a microscope (Axiovert 200M; Carl Zeiss) and IPLab software (BioVision Technologies).

Transmission electron microscopy. cLP DC/MP subsets were FACS sorted from C57BL/6 mice and resuspended in 50 μl PBS. Cell pellets from centrifuged samples were fixed overnight at 4°C with 2.5% glutaraldehyde/4% paraformaldehyde in 0.1 M sodium cacodylate buffer, pH 7.2, and then postfixed 30 min with 0.5% osmium tetroxide/0.8% potassium ferricyanide, 1 h with 1% tannic acid and overnight with 1% uranyl acetate at 4°C. Samples were dehydrated with a graded ethanol series and embedded in Spurr's resin. Thin sections were cut with an RMC MT-7000 ultramicrotome (Ventana) and stained with 1% uranyl acetate and Reynold's lead citrate before viewing at 80 kV on a transmission electron microscope (H-7500; Hitachi). Digital images were acquired with a Hammamatsu XR-100 bottom mount charge-coupled device system (Advanced Microscopy Techniques).

Bead phagocytosis assay. 3×10^6 total cLP cells were incubated for 45 min at 37°C in the presence of 75×10^6 Fluoresbrite Plain Yellow Gold 1-μm Microspheres (Polysciences Inc.) and then washed five times in cold PBS. Cells were then stained for I-Ab, CD11c, F4/80, CD11b, CD103 and CD19, CD3, TCR-β, and TCR-γδ, and the number of fluorescent microspheres in each cLP DC/MP subset was determined by flow cytometry.

Co-culture experiments

Thymidine incorporation assays. In mixed lymphocyte reactions, cLP and splenic DC/MP subsets were FACS sorted from C57BL/6 mice and co-cultured for 5 d with MACS-enriched $CD4^+$ T cells from BALB/c mouse spleens. In antigen-specific assays, FACS-sorted cLP and splenic DC/MP subsets were incubated for 2 h at 37°C in the presence of 0.5 mg/ml endotoxin-free OVA protein (EndoGrade OVA; Hyglos) and washed twice in complete RPMI before co-culture with OT-I (3 d) or OT-II cells (5 d), MACS enriched from LNs and spleen of RAG1 OT-I or RAG1 OT-II transgenic mice. In all assays, 10^5 T cells were cultured in round-bottom 96-well plates with the indicated ratios of APCs. 1 μCi $[^3H]$thymidine was added in each well for the last 18 h of culture, and thymidine incorporation was measured on a Microbeta Trilux Luminescence Counter (PerkinElmer).

T cell differentiation assays. FACS-sorted cLP or splenic DC/MP were incubated at 10^5 cells/ml for 2 h at 37°C in the presence of 0.5 mg/ml endotoxin-free OVA protein (EndoGrade OVA) and washed twice in complete RPMI before co-culture at the indicated ratios with 10^5 OT-II cells (5 d), MACS enriched from the LNs and spleen of RAG1 OT-II transgenic mice. All cultures were split and complemented with fresh media after 72 h.

On day 5, cells were restimulated for 5 h with 50 ng/ml phorbol myristate acetate and 500 ng/ml ionomycin in the presence or not of GolgiStop (BD). Cells were then surface stained with APC-Cy7–conjugated α-CD4 mAb (RM4-5) and Live/Dead Fixable cell stain kit, followed by FITC-conjugated α-foxp3 (FJK-16s), PE-conjugated α–IL-17A (eBio17B7), and APC-conjugated IFN-γ (XMG1.2) intracellular mAbs (all from eBioscience) in accordance with the manufacturer's protocol. After the 5-h restimulation period, culture supernatants were also harvested for analysis of their cytokine content.

Gene expression analysis. cLP DC/MP subsets were FACS sorted from WT C57BL/6 mice, colitic $CD45RB^{hi}$ mice, or control $CD45RB^{hi+lo}$ mice, as indicated (Figs. 1 A and 6 C), and total RNA was isolated using TRIZOL reagent (Invitrogen) according to the manufacturer's instructions. RNA quantity and quality were assessed using the 2100 Bioanalyzer (Agilent Technologies). RNA was reverse transcribed into cDNA (SuperScript III; Invitrogen), and real-time RT-PCR was performed on a 7900 HT instrument (Applied Biosystems; FAM-labeled primers were obtained from Applied Biosystems and are listed in Table S1). Gene expression was analyzed using GAPDH as

an endogenous control. In the MO-adoptive transfer experiments, gene expression analysis was performed using the TaqMan PreAmp Cells-to-Ct kit (Applied Biosystems; Denning et al., 2007a) for cDNA synthesis from a low number of cells. cDNA was then subject to a 14-cycle, target-specific preamplification step before being analyzed by regular real-time RT-PCR on a 7900 HT instrument using a custom-designed TaqMan Express Plate of 45 target genes and 3 housekeeping endogenous control genes (PN 4391526; Applied Biosystems). The main findings were confirmed by regular RT-PCR on non-preamplified cDNA.

Microarray analysis. Total RNA was extracted from biological replicates of freshly isolated, FACS-sorted cLP subsets 1–4. cDNA was prepared, labeled, and hybridized to the commercial GeneChip, mouse gene 1.0 ST containing the mouse genome for 16 h, according to standard manufacturer protocols (Affymetrix). Hybridized chips were stained and washed and were scanned using the GeneChip 3000 7Gplus scanner (Affymetrix). GeneChip Operating Software (GCOS version 1.4; Affymetrix) was used for the initial analysis of the microarray data to convert the image files to cell intensity files. All cell intensity files, representing individual biological replicates, were normalized using the RMA-sketch within Expression Console (EC version 1.1; Affymetrix) to produce the chip files and perform the quality assessment. A pivot table constructed from the individual chip files was created including calls and signal intensities for each probe set. The pivot table was then imported into GeneSpring GX 7.3 (Agilent Technologies), where hierarchical clustering using mean linkage with Pearson correlation similarity measure was used to produce the dendrogram indicating biological replicate and condition grouping. The pivot table was also imported into Genomics Suite software (Partek Inc.) to produce a principal components analysis plot as a second measure for the grouping of biological replicates. Analysis of variance was run from this dataset to produce a false discovery rate report producing multiple test-corrected p-values for each comparison of interest. The replicates of all test conditions and controls were combined, and quality filters based on combined calls, signal intensities, and fold change were used to evaluate individual probe set comparisons. Present and marginal calls were treated as the same, whereas absent calls were negatively weighted and eliminated from quality summations. Ratios of test/control values and associated analysis of variance p-values of all individual probe sets passing the above filters were summarized in Excel from GCOS, EC, GeneSpring, SAM, and Partek software. The resulting probe sets were input into Ingenuity Pathway Analysis (Ingenuity Systems) for a core analysis summarizing the genes into networks, functions, and pathways. The integrality of the microarray data is available from GEO DataSets under accession no. GSE27859.

Analysis of DC/MP and T cell cytokine production

For MP/DC cultures, culture supernatants were harvested after 24 h of culture in medium alone or LPS from *Escherichia coli* (Sigma-Aldrich). Cytokines concentrations were analyzed using the SearchLight multiplex cytokine immunoassays (Aushon Biosystems). In some cases, the amount of IL-10 was determined using a conventional double-sandwich ELISA (DuoSet mouse IL-10; R&D systems) according to the manufacturer's instructions. IFN-γ and IL-17A concentration in T cell culture supernatants (after 5 h of restimulation) was determined using conventional double-sandwich ELISA (DuoSet mouse).

BrdU incorporation experiments

WT C57BL/6 mice were pulse-injected i.p. with 0.8 mg BrdU (Sigma-Aldrich) and then continuously given 0.8 mg/ml BrdU in drinking water supplemented with 1% sucrose. cLP cell suspensions were prepared at different time points and analyzed for BrdU incorporation with the FITC–anti-BrdU Flow kit (BD).

Statistical analysis

An unpaired Student's *t* test was performed using Prism 4 software (GraphPad Software) in all cases, except for the microarray analysis (see above). Where appropriate, mean ± SD is represented on graphs. *, $P < 0.05$; **, $P < 0.01$; ***, $P < 0.001$.

Online supplemental material

Fig. S1 shows that subsets 1 and 2 have a much slower turnover than subsets 3 and 4. Fig. S2 shows that cLP subsets 3 and 4 but not 1 and 2 express CCR7 after in vitro activation. Fig. S3 shows that $F4/80^+$ cells are excluded from the organized lymphoid structures of the cLP. Fig. S4 shows that DTx treatment efficiently depletes cLP subsets 1–4 without inducing significant inflammation in the colon of CD11cDTR → C57BL/6 chimeric mice. Fig. S5 shows that the MP subsets 1 and 2 and also the $CD103^-$ DC subset 3 express E-cadherin and CX3CR1 during colitis. Table S1 lists references of the Applied Biosystems FAM-labeled primers used in this study. Table S2 shows classification of colonic MPs and DCs according to their surface marker expression and proposed functions. Online supplemental material is available at http://www.jem.org/cgi/content/full/jem.20101387/DC1.

We thank Steve Porcella and Dan Sturdevant of the Research Technologies Branch, National Institute of Allergy and Infectious Diseases (NIAID) for performing and helping to analyze the microarray data, Jason Hall and Yasmine Belkaid of the Laboratory of Parasitic Diseases, NIAID for help with T reg cell differentiation assays, and the NIAID FACS sorting facility and the Comparative Medicine Branch animal facilities for technical assistance and animal handling.

This work was supported by the Division of Intramural Research, NIAID.

The authors have no conflicting financial interests.

Submitted: 9 July 2010
Accepted: 30 November 2011

REFERENCES

Annacker, O., J.L. Coombes, V. Malmstrom, H.H. Uhlig, T. Bourne, B. Johansson-Lindbom, W.W. Agace, C.M. Parker, and F. Powrie. 2005. Essential role for CD103 in the T cell–mediated regulation of experimental colitis. *J. Exp. Med.* 202:1051–1061. http://dx.doi.org/10.1084/jem.20040662

Atarashi, K., J. Nishimura, T. Shima, Y. Umesaki, M. Yamamoto, M. Onoue, H. Yagita, N. Ishii, R. Evans, K. Honda, and K. Takeda. 2008. ATP drives lamina propria T(H)17 cell differentiation. *Nature.* 455:808–812. http://dx.doi.org/10.1038/nature07240

Bar-On, L., and S. Jung. 2010. Defining dendritic cells by conditional and constitutive cell ablation. *Immunol. Rev.* 234:76–89. http://dx.doi.org/10.1111/j.0105-2896.2009.00875.x

Bogunovic, M., F. Ginhoux, J. Helft, L. Shang, D. Hashimoto, M. Greter, K. Liu, C. Jakubzick, M.A. Ingersoll, M. Leboeuf, et al. 2009. Origin of the lamina propria dendritic cell network. *Immunity.* 31:513–525. http://dx.doi.org/10.1016/j.immuni.2009.08.010

Cheong, C., I. Matos, J.H. Choi, D.B. Dandamudi, E. Shrestha, M.P. Longhi, K.L. Jeffrey, R.M. Anthony, C. Kluger, G. Nchinda, et al. 2010. Microbial stimulation fully differentiates monocytes to DC-SIGN/CD209(+) dendritic cells for immune T cell areas. *Cell.* 143:416–429. http://dx.doi.org/10.1016/j.cell.2010.09.039

Chirdo, F.G., O.R. Millington, H. Beacock-Sharp, and A.M. Mowat. 2005. Immunomodulatory dendritic cells in intestinal lamina propria. *Eur. J. Immunol.* 35:1831–1840. http://dx.doi.org/10.1002/eji.200425882

Coombes, J.L., K.R. Siddiqui, C.V. Arancibia-Cárcamo, J. Hall, C.M. Sun, Y. Belkaid, and F. Powrie. 2007. A functionally specialized population of mucosal $CD103^+$ DCs induces $Foxp3^+$ regulatory T cells via a TGF-β– and retinoic acid–dependent mechanism. *J. Exp. Med.* 204:1757–1764. http://dx.doi.org/10.1084/jem.20070590

Denning, K.M., P.C. Smyth, S.F. Cahill, S.P. Finn, E. Conlon, J. Li, R.J. Flavin, S.T. Aherne, S.M. Guenther, A. Ferlinz, et al. 2007a. A molecular expression signature distinguishing follicular lesions in thyroid carcinoma using preamplification RT-PCR in archival samples. *Mod. Pathol.* 20:1095–1102. http://dx.doi.org/10.1038/modpathol.3800943

Denning, T.L., Y.C. Wang, S.R. Patel, I.R. Williams, and B. Pulendran. 2007b. Lamina propria macrophages and dendritic cells differentially induce regulatory and interleukin 17-producing T cell responses. *Nat. Immunol.* 8:1086–1094. http://dx.doi.org/10.1038/ni1511

Denning, T.L., B.A. Norris, O. Medina-Contreras, S. Manicassamy, D. Geem, R. Madan, C.L. Karp, and B. Pulendran. 2011. Functional specializations of intestinal dendritic cell and macrophage subsets that control Th17 and regulatory T cell responses are dependent on the T cell/APC ratio, source of mouse strain, and regional localization. *J. Immunol.* 187:733–747. http://dx.doi.org/10.4049/jimmunol.1002701

Fogg, D.K., C. Sibon, C. Miled, S. Jung, P. Aucouturier, D.R. Littman, A. Cumano, and F. Geissmann. 2006. A clonogenic bone marrow progenitor specific for macrophages and dendritic cells. *Science.* 311:83–87. http://dx.doi.org/10.1126/science.1117729

Geissmann, F., S. Jung, and D.R. Littman. 2003. Blood monocytes consist of two principal subsets with distinct migratory properties. *Immunity.* 19:71–82. http://dx.doi.org/10.1016/S1074-7613(03)00174-2

Guilliams, M., K. Movahedi, T. Bosschaerts, T. VandenDriessche, M.K. Chuah, M. Hérin, A. Acosta-Sanchez, L. Ma, M. Moser, J.A. Van Ginderachter, et al. 2009. IL-10 dampens TNF/inducible nitric oxide synthase-producing dendritic cell-mediated pathogenicity during parasitic infection. *J. Immunol.* 182:1107–1118.

Hadis, U., B. Wahl, O. Schulz, M. Hardtke-Wolenski, A. Schippers, N. Wagner, W. Müller, T. Sparwasser, R. Förster, and O. Pabst. 2011. Intestinal tolerance requires gut homing and expansion of FoxP3+ regulatory T cells in the lamina propria. *Immunity.* 34:237–246. http://dx.doi.org/10.1016/j.immuni.2011.01.016

Hapfelmeier, S., A.J. Müller, B. Stecher, P. Kaiser, M. Barthel, K. Endt, M. Eberhard, R. Robbiani, C.A. Jacobi, M. Heikenwalder, et al. 2008. Microbe sampling by mucosal dendritic cells is a discrete, MyD88-independent step in Δ*invG S. typhimurium* colitis. *J. Exp. Med.* 205:437–450. http://dx.doi.org/10.1084/jem.20070633

Iwasaki, A., and B.L. Kelsall. 1999. Freshly isolated Peyer's patch, but not spleen, dendritic cells produce interleukin 10 and induce the differentiation of T helper type 2 cells. *J. Exp. Med.* 190:229–239. http://dx.doi.org/10.1084/jem.190.2.229

Iwasaki, A., and B.L. Kelsall. 2001. Unique functions of CD11b+, CD8 alpha+, and double-negative Peyer's patch dendritic cells. *J. Immunol.* 166:4884–4890.

Iwata, M., A. Hirakiyama, Y. Eshima, H. Kagechika, C. Kato, and S.Y. Song. 2004. Retinoic acid imprints gut-homing specificity on T cells. *Immunity.* 21:527–538. http://dx.doi.org/10.1016/j.immuni.2004.08.011

Jaensson, E., H. Uronen-Hansson, O. Pabst, B. Eksteen, J. Tian, J.L. Coombes, P.L. Berg, T. Davidsson, F. Powrie, B. Johansson-Lindbom, and W.W. Agace. 2008. Small intestinal $CD103^+$ dendritic cells display unique functional properties that are conserved between mice and humans. *J. Exp. Med.* 205:2139–2149. http://dx.doi.org/10.1084/jem.20080414

Jakubzick, C., F. Tacke, F. Ginhoux, A.J. Wagers, N. van Rooijen, M. Mack, M. Merad, and G.J. Randolph. 2008. Blood monocyte subsets differentially give rise to CD103+ and CD103- pulmonary dendritic cell populations. *J. Immunol.* 180:3019–3027.

Johansson-Lindbom, B., M. Svensson, O. Pabst, C. Palmqvist, G. Marquez, R. Förster, and W.W. Agace. 2005. Functional specialization of gut $CD103^+$ dendritic cells in the regulation of tissue-selective T cell homing. *J. Exp. Med.* 202:1063–1073. http://dx.doi.org/10.1084/jem.20051100

Jung, S., D. Unutmaz, P. Wong, G. Sano, K. De los Santos, T. Sparwasser, S. Wu, S. Vuthoori, K. Ko, F. Zavala, et al. 2002. In vivo depletion of CD11c+ dendritic cells abrogates priming of CD8+ T cells by exogenous cell-associated antigens. *Immunity.* 17:211–220. http://dx.doi.org/10.1016/S1074-7613(02)00365-5

Kamada, N., T. Hisamatsu, S. Okamoto, H. Chinen, T. Kobayashi, T. Sato, A. Sakuraba, M.T. Kitazume, A. Sugita, K. Koganei, et al. 2008. Unique CD14 intestinal macrophages contribute to the pathogenesis of Crohn disease via IL-23/IFN-gamma axis. *J. Clin. Invest.* 118:2269–2280.

Laffont, S., K.R. Siddiqui, and F. Powrie. 2010. Intestinal inflammation abrogates the tolerogenic properties of MLN CD103+ dendritic cells. *Eur. J. Immunol.* 40:1877–1883. http://dx.doi.org/10.1002/eji.200939957

Liu, K., G.D. Victora, T.A. Schwickert, P. Guermonprez, M.M. Meredith, K. Yao, F.F. Chu, G.J. Randolph, A.Y. Rudensky, and M. Nussenzweig. 2009. In vivo analysis of dendritic cell development and homeostasis. *Science.* 324:392–397. http://dx.doi.org/10.1126/science.1171243

Manicassamy, S., and B. Pulendran. 2009. Retinoic acid-dependent regulation of immune responses by dendritic cells and macrophages. *Semin. Immunol.* 21:22–27. http://dx.doi.org/10.1016/j.smim.2008.07.007

Monteleone, I., A.M. Platt, E. Jaensson, W.W. Agace, and A.M. Mowat. 2008. IL-10-dependent partial refractoriness to Toll-like receptor stimulation modulates gut mucosal dendritic cell function. *Eur. J. Immunol.* 38:1533–1547. http://dx.doi.org/10.1002/eji.200737909

Mora, J.R., M. Iwata, B. Eksteen, S.Y. Song, T. Junt, B. Senman, K.L. Otipoby, A. Yokota, H. Takeuchi, P. Ricciardi-Castagnoli, et al. 2006. Generation of gut-homing IgA-secreting B cells by intestinal dendritic cells. *Science.* 314:1157–1160. http://dx.doi.org/10.1126/science.1132742

Murai, M., O. Turovskaya, G. Kim, R. Madan, C.L. Karp, H. Cheroutre, and M. Kronenberg. 2009. Interleukin 10 acts on regulatory T cells to maintain expression of the transcription factor Foxp3 and suppressive function in mice with colitis. *Nat. Immunol.* 10:1178–1184. http://dx.doi.org/10.1038/ni.1791

Naik, S.H., P. Sathe, H.Y. Park, D. Metcalf, A.I. Proietto, A. Dakic, S. Carotta, M. O'Keeffe, M. Bahlo, A. Papenfuss, et al. 2007. Development of plasmacytoid and conventional dendritic cell subtypes from single precursor cells derived in vitro and in vivo. *Nat. Immunol.* 8:1217–1226. http://dx.doi.org/10.1038/ni1522

Niess, J.H., and G. Adler. 2010. Enteric flora expands gut lamina propria CX3CR1+ dendritic cells supporting inflammatory immune responses under normal and inflammatory conditions. *J. Immunol.* 184:2026–2037. http://dx.doi.org/10.4049/jimmunol.0901936

Niess, J.H., S. Brand, X. Gu, L. Landsman, S. Jung, B.A. McCormick, J.M. Vyas, M. Boes, H.L. Ploegh, J.G. Fox, et al. 2005. CX3CR1-mediated dendritic cell access to the intestinal lumen and bacterial clearance. *Science.* 307:254–258. http://dx.doi.org/10.1126/science.1102901

Philippidis, P., J.C. Mason, B.J. Evans, I. Nadra, K.M. Taylor, D.O. Haskard, and R.C. Landis. 2004. Hemoglobin scavenger receptor CD163 mediates interleukin-10 release and heme oxygenase-1 synthesis: antiinflammatory monocyte-macrophage responses in vitro, in resolving skin blisters in vivo, and after cardiopulmonary bypass surgery. *Circ. Res.* 94:119–126. http://dx.doi.org/10.1161/01.RES.0000109414.78907.F9

Platt, A.M., C.C. Bain, Y. Bordon, D.P. Sester, and A.M. Mowat. 2010. An independent subset of TLR expressing CCR2-dependent macrophages promotes colonic inflammation. *J. Immunol.* 184:6843–6854. http://dx.doi.org/10.4049/jimmunol.0903987

Powrie, F., M.W. Leach, S. Mauze, L.B. Caddle, and R.L. Coffman. 1993. Phenotypically distinct subsets of CD4+ T cells induce or protect from chronic intestinal inflammation in C. B-17 scid mice. *Int. Immunol.* 5:1461–1471. http://dx.doi.org/10.1093/intimm/5.11.1461

Probst, H.C., K. Tschannen, B. Odermatt, R. Schwendener, R.M. Zinkernagel, and M. Van Den Broek. 2005. Histological analysis of CD11c-DTR/GFP mice after in vivo depletion of dendritic cells. *Clin. Exp. Immunol.* 141:398–404. http://dx.doi.org/10.1111/j.1365-2249.2005.02868.x

Quatresooz, P., P. Paquet, T. Hermanns-Lê, and G.E. Piérard. 2008. Molecular mapping of Factor XIIIa-enriched dendrocytes in the skin (Review). *Int. J. Mol. Med.* 22:403–409.

Rakoff-Nahoum, S., L. Hao, and R. Medzhitov. 2006. Role of toll-like receptors in spontaneous commensal-dependent colitis. *Immunity.* 25:319–329. http://dx.doi.org/10.1016/j.immuni.2006.06.010

Read, S., V. Malmström, and F. Powrie. 2000. Cytotoxic T lymphocyte–associated antigen 4 plays an essential role in the function of $CD25^+CD4^+$ regulatory cells that control intestinal inflammation. *J. Exp. Med.* 192:295–302. http://dx.doi.org/10.1084/jem.192.2.295

Rescigno, M., M. Urbano, B. Valzasina, M. Francolini, G. Rotta, R. Bonasio, F. Granucci, J.P. Kraehenbuhl, and P. Ricciardi-Castagnoli. 2001. Dendritic cells express tight junction proteins and penetrate gut epithelial monolayers to sample bacteria. *Nat. Immunol.* 2:361–367. http://dx.doi.org/10.1038/86373

Rogler, G., M. Hausmann, D. Vogl, E. Aschenbrenner, T. Andus, W. Falk, R. Andreesen, J. Schölmerich, and V. Gross. 1998. Isolation and phenotypic characterization of colonic macrophages. *Clin. Exp. Immunol.* 112:205–215. http://dx.doi.org/10.1046/j.1365-2249.1998.00557.x

Rugtveit, J., E.M. Nilsen, A. Bakka, H. Carlsen, P. Brandtzaeg, and H. Scott. 1997. Cytokine profiles differ in newly recruited and resident subsets of mucosal macrophages from inflammatory bowel disease. *Gastroenterology*. 112:1493–1505. http://dx.doi.org/10.1016/S0016-5085(97)70030-1

Sawatani, Y., T. Miyamoto, S. Nagai, M. Maruya, J. Imai, K. Miyamoto, N. Fujita, K. Ninomiya, T. Suzuki, R. Iwasaki, et al. 2008. The role of DC-STAMP in maintenance of immune tolerance through regulation of dendritic cell function. *Int. Immunol.* 20:1259–1268. http://dx.doi.org/10.1093/intimm/dxn082

Schledzewski, K., M. Falkowski, G. Moldenhauer, P. Metharom, J. Kzhyshkowska, R. Ganss, A. Demory, B. Falkowska-Hansen, H. Kurzen, S. Ugurel, et al. 2006. Lymphatic endothelium-specific hyaluronan receptor LYVE-1 is expressed by stabilin-1+, F4/80+, CD11b+ macrophages in malignant tumours and wound healing tissue in vivo and in bone marrow cultures in vitro: implications for the assessment of lymphangiogenesis. *J. Pathol.* 209:67–77. http://dx.doi.org/10.1002/path.1942

Schulz, O., E. Jaensson, E.K. Persson, X. Liu, T. Worbs, W.W. Agace, and O. Pabst. 2009. Intestinal $CD103^+$, but not $CX3CR1^+$, antigen sampling cells migrate in lymph and serve classical dendritic cell functions. *J. Exp. Med.* 206:3101–3114. http://dx.doi.org/10.1084/jem.20091925

Sica, A., P. Allavena, and A. Mantovani. 2008. Cancer related inflammation: the macrophage connection. *Cancer Lett.* 267:204–215. http://dx.doi.org/10.1016/j.canlet.2008.03.028

Siddiqui, K.R., S. Laffont, and F. Powrie. 2010. E-cadherin marks a subset of inflammatory dendritic cells that promote T cell-mediated colitis. *Immunity*. 32:557–567. http://dx.doi.org/10.1016/j.immuni.2010.03.017

Smith, P.D., L.E. Smythies, M. Mosteller-Barnum, D.A. Sibley, M.W. Russell, M. Merger, M.T. Sellers, J.M. Orenstein, T. Shimada, M.F. Graham, and H. Kubagawa. 2001. Intestinal macrophages lack CD14 and CD89 and consequently are down-regulated for LPS- and IgA-mediated activities. *J. Immunol.* 167:2651–2656.

Smythies, L.E., M. Sellers, R.H. Clements, M. Mosteller-Barnum, G. Meng, W.H. Benjamin, J.M. Orenstein, and P.D. Smith. 2005. Human intestinal macrophages display profound inflammatory anergy despite avid phagocytic and bacteriocidal activity. *J. Clin. Invest.* 115:66–75.

Sun, C.M., J.A. Hall, R.B. Blank, N. Bouladoux, M. Oukka, J.R. Mora, and Y. Belkaid. 2007. Small intestine lamina propria dendritic cells promote de novo generation of Foxp3 T reg cells via retinoic acid. *J. Exp. Med.* 204:1775–1785. http://dx.doi.org/10.1084/jem.20070602

Takada, Y., T. Hisamatsu, N. Kamada, M.T. Kitazume, H. Honda, Y. Oshima, R. Saito, T. Takayama, T. Kobayashi, H. Chinen, et al. 2010. Monocyte chemoattractant protein-1 contributes to gut homeostasis and intestinal inflammation by composition of IL-10-producing regulatory macrophage subset. *J. Immunol.* 184:2671–2676. http://dx.doi.org/10.4049/jimmunol.0804012

Takeda, K., B.E. Clausen, T. Kaisho, T. Tsujimura, N. Terada, I. Förster, and S. Akira. 1999. Enhanced Th1 activity and development of chronic enterocolitis in mice devoid of Stat3 in macrophages and neutrophils. *Immunity*. 10:39–49. http://dx.doi.org/10.1016/S1074-7613(00)80005-9

Vallon-Eberhard, A., L. Landsman, N. Yogev, B. Verrier, and S. Jung. 2006. Transepithelial pathogen uptake into the small intestinal lamina propria. *J. Immunol.* 176:2465–2469.

Varol, C., A. Vallon-Eberhard, E. Elinav, T. Aychek, Y. Shapira, H. Luche, H.J. Fehling, W.D. Hardt, G. Shakhar, and S. Jung. 2009. Intestinal lamina propria dendritic cell subsets have different origin and functions. *Immunity*. 31:502–512. http://dx.doi.org/10.1016/j.immuni.2009.06.025

Weber, B., L. Saurer, M. Schenk, N. Dickgreber, and C. Mueller. 2011. CX3CR1 defines functionally distinct intestinal mononuclear phagocyte subsets which maintain their respective functions during homeostatic and inflammatory conditions. *Eur. J. Immunol.* 41:773–779. http://dx.doi.org/10.1002/eji.201040965

Worbs, T., U. Bode, S. Yan, M.W. Hoffmann, G. Hintzen, G. Bernhardt, R. Förster, and O. Pabst. 2006. Oral tolerance originates in the intestinal immune system and relies on antigen carriage by dendritic cells. *J. Exp. Med.* 203:519–527. http://dx.doi.org/10.1084/jem.20052016